A high-resolution temporal record of environmental changes in the Eastern Caribbean (Guadeloupe) from 40 to 10 ka BP

Aurélien Royer, Bruno Malaizé, Christophe Lécuyer, Alain Queffelec, Karine Charlier, Thibaut Caley, Arnaud Lenoble

A high-resolution temporal record of environmental changes in the Eastern Caribbean (Guadeloupe) from 40 to 10 ka BP

Aurélien Royer[a], Bruno Malaizé[b], Christophe Lécuyer[c,d], Alain Queffelec[a], Karine Charlier[b], Thibaut Caley[b], Arnaud Lenoble[a]

[a] Université de Bordeaux, CNRS UMR 5199 PACEA, Bâtiment B18, Allée Geoffroy Saint Hilaire, CS 50023, 33615 Pessac Cedex, France

[b] Université de Bordeaux, CNRS UMR 5805 EPOC, Bâtiment B18, Allée Geoffroy Saint Hilaire, CS 50023, 33615 Pessac Cedex, France

[c] Université Lyon 1, CNRS UMR 5276 Laboratoire de Géologie de Lyon, et Ecole Normale Supérieure de Lyon, 69622 Villeurbanne, France d Institut Universitaire de France, Paris, France

Abstract

In neotropical regions, fossil bat guano accumulated over time as laminated layers in caves, hence providing a high-resolution temporal record of terrestrial environmental changes. Additionally, cave settings have the property to preserve such organic sediments from processes triggered by winds (deflation, abrasion and sandblasting) and intense rainfall (leaching away). This study reports both stable carbon and nitrogen isotope compositions of frugivorous bat guano deposited in a well-preserved stratigraphic succession of Blanchard Cave on Marie-Galante, Guadeloupe. These isotopic data are discussed with regard to climate changes and its specific impact on Eastern Caribbean vegetation during the Late Pleistocene from 40 to 10 ka cal. BP. Guano $\delta^{13}C$ values are higher than modern ones, suggesting noticeable vegetation changes. This provides also evidence for overall drier environmental conditions during the Pleistocene compared to today. Meanwhile, within this generally drier climate, shifts between wetter and drier conditions can be observed. Large temporal amplitudes in both $\delta^{13}C$ and $\delta^{15}N$ variations reaching up to 5.9‰ and 16.8‰, respectively, also indicate these oceanic tropical environments have been highly sensitive to regional or global climatic forcing. Stable isotope compositions of bat guano deposited from 40 to 35 ka BP, the Last Glacial Maximum and the Younger-Dryas reveal relatively wet environmental conditions whereas, at least from the end of the Heinrich event 1 and the Bølling period the region experienced drier environmental conditions. Nevertheless, when considering uncertainties in the model age, the isotopic record of Blanchard Cave show relatively similar variations with known proxy records from the northern South America and Central America, suggesting thus that the Blanchard Cave record is a robust proxy of past ITCZ migration. Teleconnections through global atmospheric pattern suggest that islands of the eastern Caribbean Basin could be also under the influence of a bipolar temperature gradients that impact the mean location of the ITCZ, with a Southern Hemisphere imprint during the glacial period and a more significant role of Northern Hemisphere during the last deglaciation.

Keywords : Caribbean Basin ; Last Glacial ; Guano ; Carbon isotope

1. Introduction

Evidence for abrupt and short climate changes prevailing during the late Quaternary are widespread in both marine and terrestrial archives (Bond et al., 1993; Dansgaard et al., 1993; Wang et al., 2001). These records have notably revealed a complex climate system, including close relationships between the two

hemispheres (e.g. Charles et al., 1996; Blunier and Brook, 2001) as well as between high and low latitudes (e.g. Peterson et al., 2000; Haug et al., 2001; Lea et al., 2003; Schmidt et al., 2004, 2012; Deplazes et al., 2013). For tropical regions, past climate conditions were strongly influenced by the position and migration of the InterTropical Convergence Zone (ITCZ), which is linked to modifications of the Atlantic Meridional Overturning Circulation (AMOC), sea-ice expansion in the North Atlantic and pole-to-equator gradient of sea surface temperatures (e.g. Broccoli et al., 2006; Stouffer et al., 2006). Consequently, climate variability deduced from the late Quaternary archive of the Caribbean Basin has been considered as related to meridional displacements of the mean ITCZ position (e.g. Peterson and Haug, 2006; Hodell et al., 2008) (Fig. 1). In fact, the current climate mode of the Caribbean region is strongly influenced by seasonal changes in the displacement of the ITCZ as well as by the Bermuda-Azores high-pressure systems located in the North Atlantic that either maintain or reduce zonal trade winds. The present-day climate of this area is characterized by an annual cycle of rainfall exhibiting a bimodal structure with two rainfall maxima running from May to November, when the ITCZ shifts north of the equator, separated by a mid-summer drought in JulyeAugust (Giannini et al., 2000). However, each region of the Caribbean Basin is characterized by a distinct climate mode (Gamble et al., 2008). For example, southern areas are influenced by the Caribbean LowLevel Jet (Gamble and Curtis, 2008), while the Eastern Caribbean area is mostly influenced by the synoptic variability of the thermohaline circulation, as well as the Bermuda-Azores high-pressure systems and the North Atlantic Oscillation (NAO) (Giannini et al., 2001; Gamble and Curtis, 2008; Gamble et al., 2008).

Any attempt to investigate climate variability and its impact on both flora and fauna assemblages in the terrestrial domains of the Caribbean Islands remains challenging mainly due to the scarcity of Late Quaternary sedimentary records. Thus far, terrestrial climate records are primarily recovered from lacustrine and cave deposits. Lacustrine deposits allow for the analysis of sedimentary structures and textures (Street-Perrott et al., 1993; Bertran et al., 2004), the determination of pollen (Leyden,1995; Bush et al., 2009; Lane et al., 2009) and ostracod assemblages (Hodell et al., 1991; Curtis and Hodell, 1993; Holmes, 1998), as well as the stable isotope analysis of aquatic invertebrates and sedimentary organic matter (Beets et al., 2006; Malaize et al., 2011; Yanes and Romanek, 2013). However, most shallow lakes in Central America and the Caribbean were dry during the last glacial period as tropical lakes are highly sensitive to changes in the balance between precipitation and evaporation. Nevertheless, sedimentary deposits in cave contexts can preserve speleothems (e.g. Lachniet et al., 2004; Fensterer et al., 2013; Gazquez et al., 2013; Lachniet et al., 2013) and fossil bones (e.g. Pregill et al., 1994; Lenoble et al., 2009; Bochaton et al., 2015; Stoetzel et al., 2016) as well as fossil bat guano, which may constitute climate archives over periods exceeding several thousand years (Des Marais et al.,1980; Mizutani et al.,1992a,b; Wurster et al., 2008). Indeed, continuous accumulations of laminated bat guano, which can extend from recent periods to beyond the Last Glacial Maximum (McFarlane et al., 2002; Bird et al., 2007; Wurster et al., 2008, 2010a; Onac et al., 2014, 2015; Forray et al., 2015; Widga and Colburn, 2015; Choa et al., 2016; Cleary et al., 2016), provide a high temporal resolution record of environmental changes (Wurster et al., 2007).

The purpose of this study is to evaluate the impact of past climatic changes on tropical eastern Caribbean environments, especially high-frequency fluctuations in precipitation that can be estimated from both carbon and nitrogen isotope compositions of fossil bat guano sampled from Blanchard Cave,

Marie-Galante Island. The high temporal resolution of past environmental changes observed due to laminated structure of the guano is compared with others proxies (Cariaco Basin, Peten Itz a, polar ice cores from Greenland and Antarctica) to discuss potential teleconnections between tropical and polar regions.

2. The Blanchard Cave: location and stratigraphy

Marie-Galante is a carbonate flat island (maximal elevation of 204 m) belonging to the Guadeloupe archipelago. This small island is located on a separate bank isolated from Guadeloupe, even during glacial lowstands. The archipelago experiences a tropical climate where rainy (JuneeNovember) and dry (DecembereMay) seasons alternate with slight variations in temperature (mean annual temperature of 27 C). Due to the low relief of the island, Marie-Galante receives limited precipitation (maximal annual rain fall of around 1500 mm). The present-day environmental conditions on Marie-Galante result from a profound alteration of the landscape by historical crops such as tobacco, coffee, cotton, sugar cane and indigo (Rousteau et al., 1996). The eastern coast of the island is arid, hosting dry scrub forests and deciduous dry forests further inland whereas swamps are mainly present along the northwestern coast. The middle part of the island is characterized by ravines that host a slightly moister vegetation than the surroundings (Lasserre, 1961; Portecop, 1982; Rousteau et al., 1996).

Blanchard Cave is a flank margin cave currently located 200 m from the southern coastline of Marie-Galante Island, near the village of Capesterre (155205600N; 611400100O) (Lenoble et al., 2009). Its distance from the shore slightly varied in the past (Fig. 1b). The cave morphology is constituted of a corridor around 35 m length, 5e8 m wide and 6e7 m high that opens at the base of a fossil cliff 200 m from the sea (Fig. 1). The cave was dug into PlioPleistocene neritic limestones (Bouysse et al.,1993) and was further shaped during the high sea-level stand of the last Interglacial MIS 5 (125 ka) (Lenoble et al., 2009).

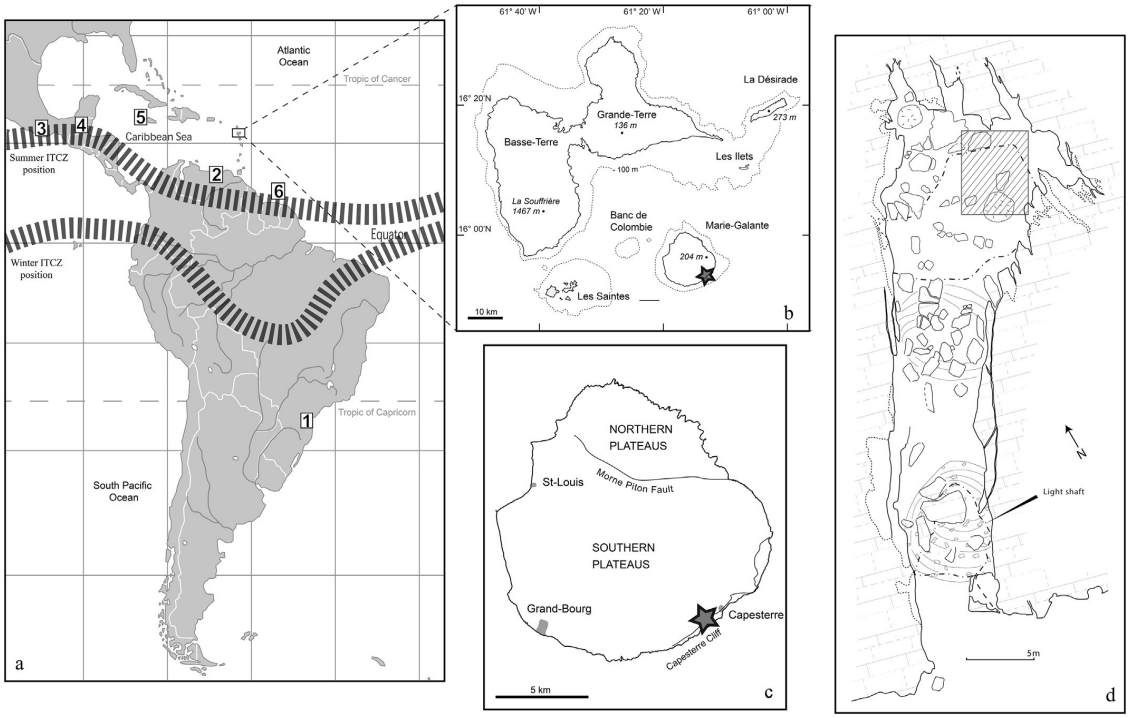

Fig. 1. Topographic maps of the Caribbean Basin and the South America (a) and Guadeloupe Islands showing the modification of coastline subsequent to a 100 m sea-level fall (b), and the geographic location of Blanchard Cave (black star) in Marie-Galante Island (c), as well as the topographic map of the cave (d). The grey hatched area in Fig. 1D indicates the location of the excavation. The hatched line in Fig. 1A indicates the extent summer and winter position of the ITCZ. Numbers refer to sites mentioned in the text: 1) Botuvera cave, 2) Cariaco Basin, 3) Juxtlahuaca Cave, 4) Lake Peten Itz a, 5) Lake Wallywash Great Pond, and 6) MD03-2616.

The large openness of the cave (~5 m wide) makes it clearly identifiable in the landscape and explains why it has been referred to various names over time: Grotte Madame Lionel (Lasserre,1961), Grotte Caraïbe (Barbotin, 1987), Voûte a Quinquins (Rodet, 1987), and Grotte Toto (Stouvenot, 2003). In 2005, a survey work performed at the cave entrance revealed an archaeological layer dated to the Pre-Columbian period (Stouvenot, 2005; Grouard et al., 2013). In 2008, a 2 m deep test pit was dug in the far end of the cave with palaeontological excavations in 2013 and 2014. This test documents, under a thin layer of modern bat guano

(thickness < 0.1 m), an important stratigraphy divided into twelve fossil-bearing layers overlying the bedrock (Fig. 2), which deliver faunal fossil remains (Bailon et al., 2015; Gala and Lenoble, 2015; Stoetzel et al., 2016). These twelve levels can be classified into five sedimentary facies:

Level 1 is made of massive beige silts slightly cemented forming the uppermost part of the cave infilling.

Level 2 is constituted of massive brown silts containing more or less residual organic matter.

Levels 3, 5, 8,10 and 12 are composed of brown silt-size organicrich brown sediments derived from vegetal remains defecated primarily by fruit bats. These levels are characterized by laminated deposits themselves intercalated with authigenic phosphate minerals. The observation of thin sections under a microscope revealed that these silts were formed by the accumulation of laminated and partially altered organic debris despite the occasional presence of vegetal material (Fig. 3b and c).

Levels 6, 7, 9 and 11 are formed of silts similar to those occurring in the previous facies but characterized by a massive structure including limestones debris. Under the microscope, samples from these levels exhibit numerous bioturbation patterns measuring of several centimeters in diameter generated by burrowing organisms attesting to the reworking of these deposits (Fig. 3a). Due to these bioturbation patterns, we have chosen to collect in each level samples that average 5 cm thickness of level deposit.

Level 4 is constituted of a pile of blocks with voids filled by micro-laminated carbonated sands that most likely result from a single roof collapse event.

Mineralogical and chemical characterizations of the deposit (organic matter, sulfur, and carbonate content, pH) indicate that these sedimentary changes do not correlate with major variations in sediment composition throughout the sequence, apart from level 4 functioning as a carbonate buffer due to its limestone debris content (cf. Suppl. material S1).

Hygric measurements have demonstrated that Blanchard Cave is a dry cave throughout the year, with frequent air circulation caused by a decrease in outside temperatures, leading to the arrival of cold air in the cave and an interruption in the thermal stratification of the ambient air (Lenoble et al., 2015). Due to these microclimate parameters, Blanchard Cave is considered as a cool chamber following the classification of bat roosting sites in the Caribbean (e.g. Rodríguez-Duran, 2010). Currently and all the year round, the cave entrance is home of a couple of harems, each composed of a dozen Jamaican fruit-eating bats (Artibeus jamaicensis), a frugivorous species belonging to the Phyllostomidae family. The far end of the cave, which hosts a colony of Antillean fruit-eating bats (Brachyphylla cavernarum), mainly functions as a nursery roost occupied seasonally. Fossil remains of the Antillean fruit-eating bat have been retrieved throughout the deposit, associated with remains of three others frugivorous or nectarivorous species found in less extent (Stoetzel et al., 2016).

No insect remains have thus far been recovered from any part of the sequence, despite a careful examination under binocular of several samples throughout the infilling. That is somewhat surprising for two reasons. First, the Antillean fruit bat has a less restrictive diet compared to other frugivorous species, enabling them to consume higher proportions of insects in some circumstances (Bond and Seaman, 1958; Soto-Centeno et al., 2001; Lenoble et al., 2014). Second, bones referable to eight insectivore species are found associated with Antillean fruit bat through the whole sequence. Such observation does not exclude, however, a contribution of insect accumulation to the deposit formation despite the well-preserved organic matter.

A

B

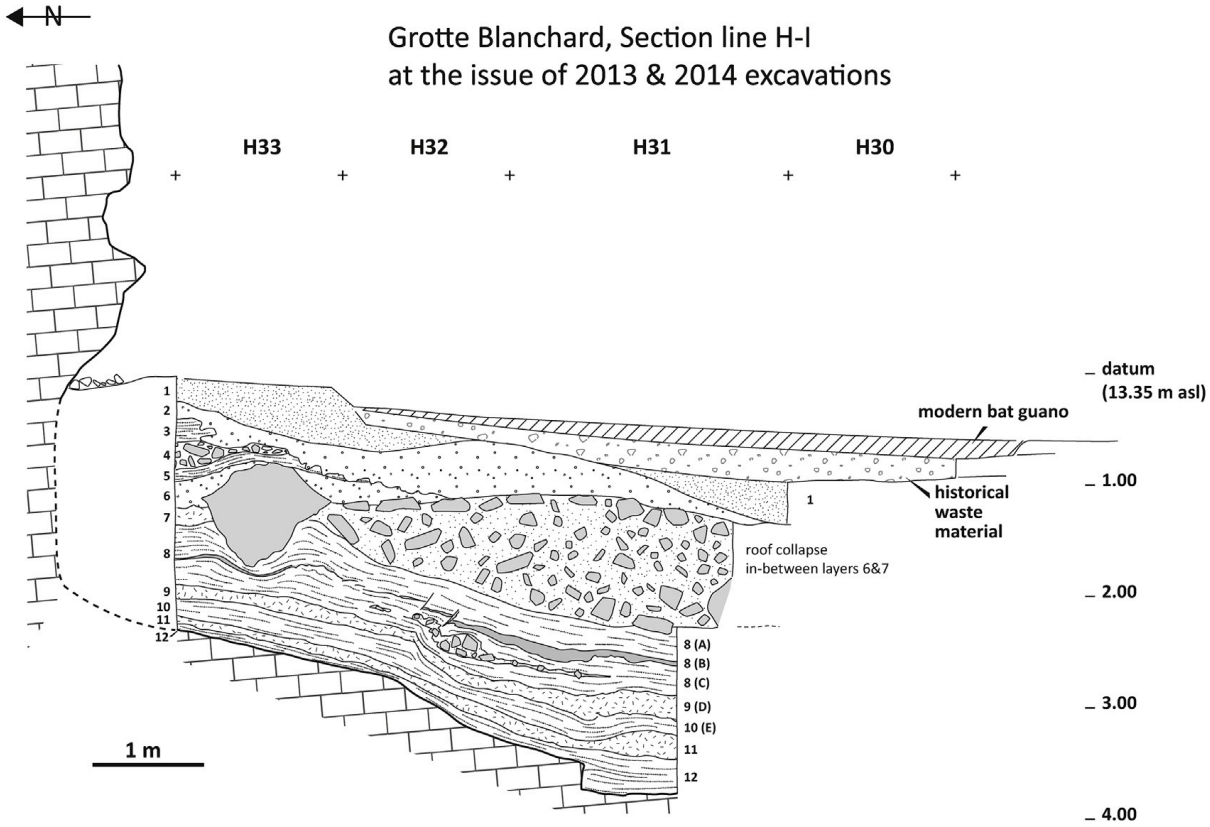

Fig. 2. Sedimentary deposits of the Blanchard Cave, (A) photography, (B) schematic representation.

3. Methods

3.1. Sampling method

Guano samples were directly collected from throughout the stratigraphic sequence. Levels 3 to 11 were sampled in the northern part of the sequence (square H33 - Fig. 2), whereas level 12 was sampled in the southern part (square H31), where this particular level is more clearly identifiable. The depth of the level 12 top was corrected to correspond to the base of the level 11. Samples from levels 3, 5, 8,10 and 12 comprise 2-4 mm of sediment continuously collected according to sedimentary levels inclination and lamination. As levels 6, 7, 9 and 11 are massive deposits, bulk samples were defined at the scale from 2 to 5 cm and they have been considered as mean points averaging isotopic signatures of the levels, in which they come from. In addition, a sample of modern guano collected in 2012 was analyzed in order to have a present-day reference for both d13C and d15N values.

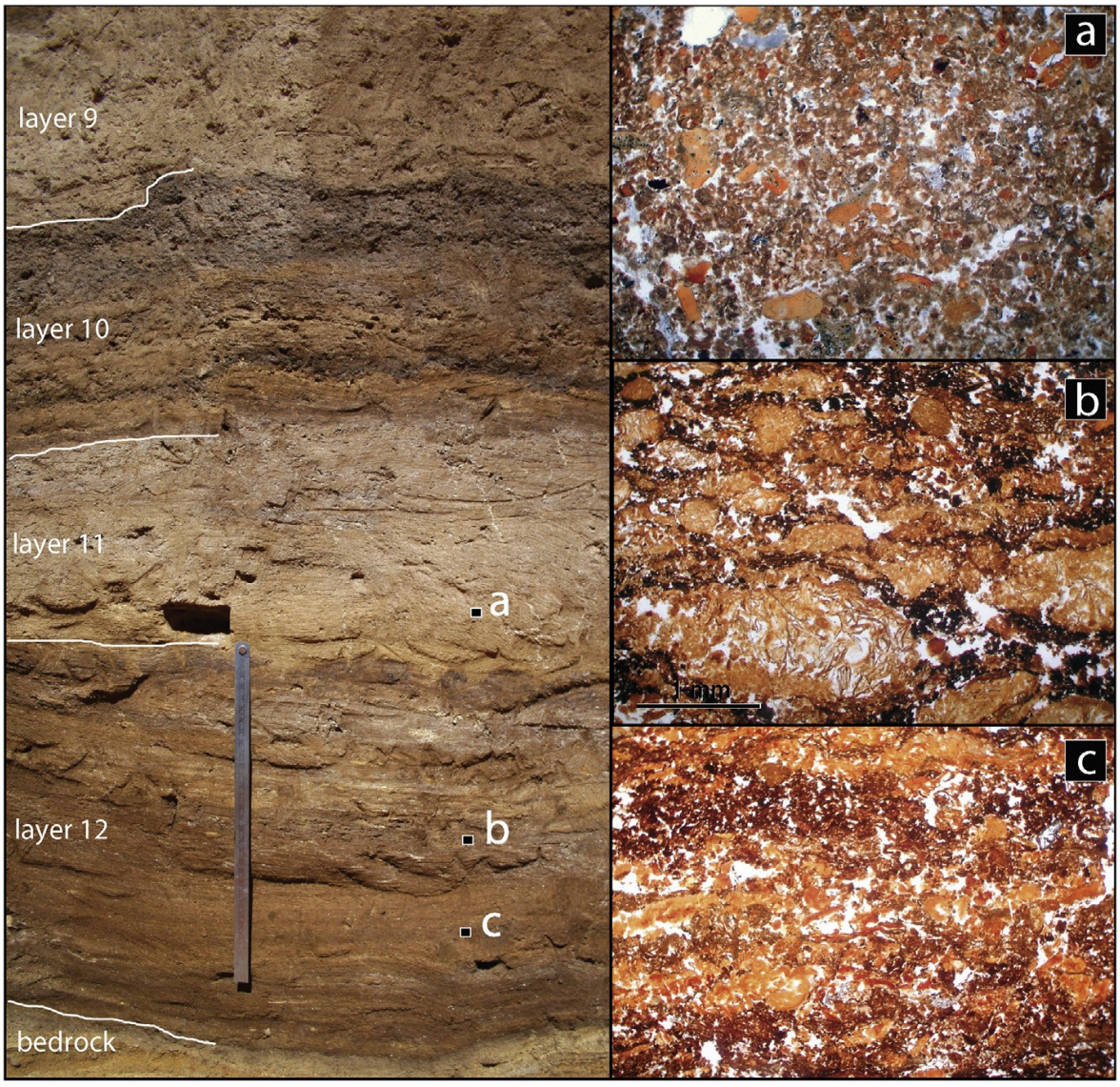

Fig. 3. Sedimentary facies of fossil guano constituting the Blanchard Cave infilling. Illustrated at left: bedded deposit with alternating massive (levels 9, 11) and laminated beds (levels 10, 12), with the scale given by the 30-cm-ruler. At right: micro-facies with (a) micro-aggregated sediment mixed by bioturbation forming massive layers, (b) organic laminated sediment including flattened yellowish aggregates assumed to represent fruit-bat droppings, and (c) phosphatized laminae (bright red) intercalated within laminated organic sediment, both sedimentary facies encountered in laminated layers.

3.2. Radiocarbon dates and age modeling

Sixteen samples of fossil guano were sent for AMS 14C dates by the three institutes: Vienna Institute for Isotopes and Nuclear Physics, Austria, which operated MeOH washing and acid-base-acid protocol; the laboratory of Groenigen, Netherlands, and the Artemis AMS laboratory in Saclay, France (Table 1), which have just pretreated samples with HCl acid to avoid any alteration of organic matter with basic treatment. The reported dates were calibrated at 3s (99.7%) using the IntCal13 calibration curve (Reimer et al., 2013). Nine of these dates match individual samples (samples from Groeningen and Vienna). The seven remaining dates were obtained from Artemis before the high resolution sampling conducted for isotopic analyses to evaluate the stratigraphy. They correspond to five to ten samples, conducting thus to engender larger confidence intervals in the age model compared to the first set of dates from Groeningen and Vienna (Table 1).

The age-depth model was generated by using in the R-CRAN software (R Development Core Team, 2008) the 'Classical age-depth modeling' (Clam software version 2.2) developed by Blaauw (2010) and by applying a linear regression to the data (Fig. 4). Dates range from the top of level 3 to the middle part of level 12 while extrapolated ages were assigned to the last twenty-five samples from level 12. As level 4 is a roof collapse, it was considered as an instantaneous event. With the exception of level 4, the mean accumulation rate is estimated at 0.06 mm/year, suggesting that each sample represents 50 ± 15 years. Dehydration and compaction effects can explained this low rate of accumulation, as well as an irregular occupation of the cave by bats. Age uncertainties at 99.7% in this age-depth model are less than 1.8 ka.

Laboratory	Ref-labo	Unit	Depth (mm)	Age 14 C yr BP	S. dev. (1s)	IntCal09 min BP	IntCal09 max BP
Vienna	A/GB-13-13	3	573 ± 1.25	8999	313	9014	11404
Artemis	Lyon-5726 (SacA-14261)	3	576.25 ± 10	9740	50	10789	11270
Vienna	A/GB-13-59	3	676 ± 1.25	9291	351	9400	12238
Vienna	A/GB-13-63	5	984 ± 1.5	10005	335	10249	12805
Artemis	Lyon-6976 (SacA 19445)	5	997 ± 16.5	10690	70	12421	12750
Vienna	A/GB-13-113	5	1106.5 ± 1.5	11348	285	12429	14195
Artemis	Lyon-6977 (SacA 19446)	6	1344 ± 137	14010	80	16546	17452
Vienna	A/GB-13-117	8	1457 ± 1	15081	447	16786	19958
Artemis	Lyon-6978 (SacA 19447)	8	1704.75 ± 16.25	19940	150	23427	24530
Artemis	Lyon-6979 (SacA 19448)	8 base	1894.5 ± 20.75	23200	220	26764	27960
Artemis	Lyon-8497 (SacA 26110)	10	2052 ± 20	25320	220	28663	30400
Artemis	Lyon-8498 (SacA 26111)	10	2196 ± 24	25300	220	28649	30374
Vienna	A/GB-13-387	10	2220 ± 1.25	26539	196	30154	31227
Artemis/Groeningen	Lyon-11133(Gra) /GB-14-409	10	2279.25 ± 2	27510	140	30988	31717
Artemis/Groeningen	Lyon-11134(Gra)/GB-14-445	12	2426 ± 1	31150	180	34517	35698
Artemis/Groeningen	Lyon-11135(Gra) /GB-14-499	12	2596.5 ± 1.5	34640	230	38440	40004

Table 1 Radiocarbon dates obtained on organic matter from bat Guano (Blanchard Cave, Marie-Galante, Guadeloupe). Dates are calibrated at 3s (99.7%) using the calibration curve IntCal13 (Reimer et al., 2013). Depth (mm) is expressed in function of the datum level.

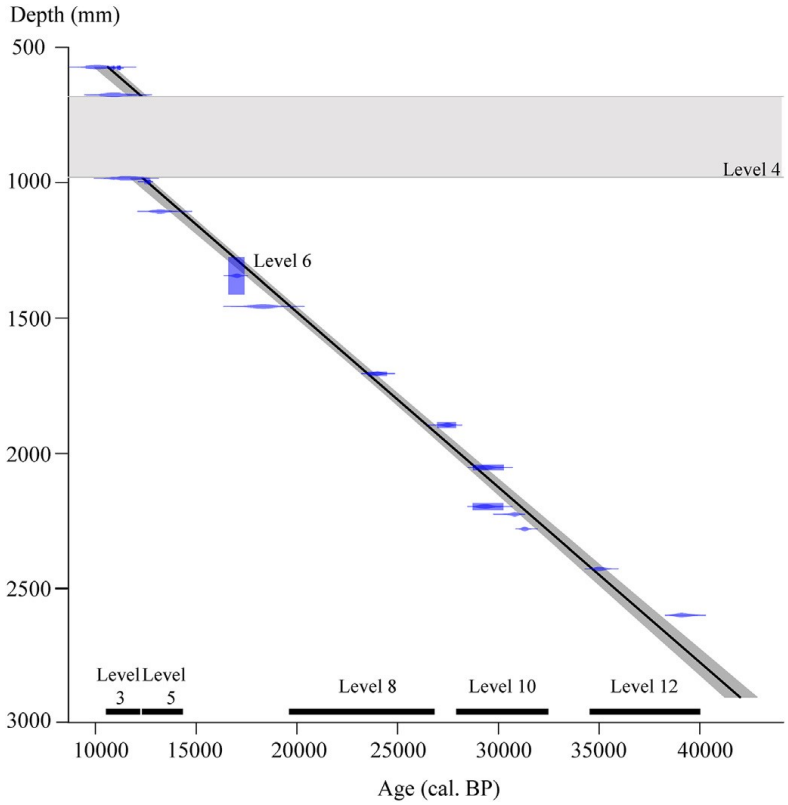

Fig. 4. Age-depth model and radiocarbon dates calibrated using Clam software v2.2 (Blaauw, 2010). The grey area defines the 99.7% confidence envelope.

	$\delta^{13}C$ values				$\delta^{15}N$ values			
	n	Mean	Minimum	Maximum	n	Mean	Minimum	Maximum
Modern Guano	1	−27.0	–	–	1	11.1	–	–
Level 3	23	−25.1	−25.6	−24.6	23	17.4	14.9	19.0
Level 4	1	−24.7	–	–	1	15.1	–	–
Level 5	26	−22.0	−25.5	−20.4	26	21.1	16.4	22.2
Level 6	2	−20.3	−20.4	−20.2	2	22.3	22.0	22.7
Level 7	3	−22.8	−23.3	−21.9	3	14.2	12.1	17.4
Level 8	93	−24.0	−24.9	−22.2	93	14.0	7.7	18.7
Level 9	1	−22.5	–	–	1	11.7	–	–
Level 10	51	−24.6	−25.4	−23.7	50	8.8	6.8	11.1
Level 11	1	−24.7	–	–	–	–	–	–
Level 12	54	−24.5	−25.7	−19.8	30	9.7	6.0	18.5
TOTAL fossil	255	−24.1	−25.7	−19.8	229	13.5	6.0	22.7

Table 2. Mean, minimal and maximal values of carbon and nitrogen isotope compositions from modern and fossil guano recovered from the sedimentary accumulations preserved in Blanchard Cave, Marie-Galante, Guadeloupe.

3.3. Stable isotope measurements

Carbon and nitrogen isotope ratios were measured from a subset of guano samples collected, with 255 and 229 samples, respectively (Table 2; Suppl. material S2). Each sample was sieved with a 500 mm mesh and decarbonated using an 8% hydrochloric acid solution for 12 h at 90 C in order to remove limestone bedrock particles before being washed with deionized water and dried at low temperature. Aliquots of guano samples from 0.5 to 2.0 mg were loaded into tin capsules and analyzed with an isotope ratio mass spectrometer (IsoPrime GV Instruments®) interfaced with an Elemental Analyzer (EA; Flash2000, ThermoFisher®) at the EPOC Laboratory of the University of Bordeaux, France. Daily drift of isotopic measurements was corrected using a series of internal isotopic references (acetanilide C8H9NO, casein C47H48N3NaO7S2, glycin C2H5NO2). Stable isotope ratios are expressed in the conventional delta notation as parts per thousand (‰) deviations from the Vienna Pee Dee Belemnite (V-PDB) international standards for d13C and atmospheric N2 for d15N. Analysis

uncertainty was better than 0.3‰ for d15N and 0.2‰ for d13C. Duplicate measurements were performed for 81 samples.

3.4. Interpretation of carbon and nitrogen isotope compositions of bat guano

Carbon and nitrogen isotope compositions of fossil animal derived organic remains, such as bones, dung and guano, are commonly used to reconstruct palaeoenvironments. The underlying basis of stable isotope investigations on animal organic remains is that 1) there are isotopic relationships within the biosphere and geosphere due to fractionation taking place during natural chemical and physical processes. This results in isotopic differences between different foods consumed; and 2) climatic parameters can affect fractionation during these processes, thus modifying the isotopic signatures of the diet. These isotopic signatures are recorded during the absorption and incorporation of food in both the consumer tissues (e.g. De Niro and Epstein, 1981; Kelly, 2000) and feces (Herrera et al., 2001a, 2001b; Painter et al., 2009; SotoCenteno et al., 2014). Thus, changes in climate are recorded in the isotopic signatures of animal body tissues and feces.

The primary control on plant $\delta^{15}N$ values is their ability to use nitrogen, which is absorbed directly from the atmosphere through symbiotic soil bacteria for leguminous plants or from soil nitrate for non-leguminous plants. At the global scale, $\delta^{15}N$ values of soils and plants decrease with the reduction of mean annual temperature and the increase of mean annual precipitation (Amundson et al., 2003), both being climatic factors that ultimately control the biological activity and the soil nitrogen cycling. This assumption led many scientists to use $\delta^{15}N$ variation of fossil animal organic remains as a proxy of the amount of precipitation. However, it is important to note that plant $\delta^{15}N$ values can vary seasonally up to several per mil, and also depend on plant segments (Kolb and Evans, 2002), and between various plant taxa occurring in the same site (Handley et al., 1999). Such complexity, related to the simultaneous participation of processes of isotope fractionation operating within the nitrogen cycle, generally produces weak statistical relationships between plant $\delta^{15}N$ values and considered climate factors (Amundson et al., 2003; Murphy and Bowman, 2006, 2009; Makarov, 2009).

Carbon isotope compositions of plants mainly depend on metabolic pathways for assimilating atmospheric carbon (i.e. plants C3, C4 and CAM), which is more or less modulated by local environmental parameters such as water stress, CO_2 partial pressure, exposure to sunlight and openness of the vegetation. Changing vegetation patterns in bat foraging areas (from 5 to 20 km) are recorded in both carbon and nitrogen isotope compositions of insectivorous bats (Wurster et al., 2007) and phytophageous (Royer et al., 2015) bat feces. The digesta of insectivorous and phytophageous bats is quickly transited in a few hours or less without undergoing radical changes in the gastrointestinal tract (Morrison, 1980; Painter et al., 2009). The isotopic carbon difference between bat diet and their feces was estimated by Salvarina et al. (2013) to be 0.11 ± 0.8‰ and by Des Marais et al. (1980) as close to 0.8‰, respectively. Consequently, in the case of phytophageous bats, it can be assumed that this isotopic fractionation is close to zero and that stable isotope compositions of their feces directly reflect those of the plants consumed. Past climatic and environmental changes can influence isotopic compositions of feces as bats modify their diet to changes in the diversity and abundance of local resources, including the ratio between C4 and C3 plants.

Distinct strategies of carbon fixation among plants allowed the determination of a range of $\delta^{13}C$ values comprised between 36 and 22‰ for C3 while C4 are less ^{13}C-depleted relative to their CO_2 source with values ranging from 15 to 10‰ (Bender, 1971; Smith and Epstein, 1971). Internal variations in $\delta^{13}C$ values for photosynthetic plants result from local conditions including ambient light conditions, temperature, pCO_2 and water availability (e.g. Smith et al., 1976; Farquhar et al., 1989; Ehleringer et al., 1997; Kohn, 2010). For example, subcanopy C3 plants, which grow in humid and shaded environments, have lower $\delta^{13}C$ values than those growing in arid and open environments. Studies have shown that part

of the $\delta^{13}C$ variability of C3 plants is influenced by local precipitation, and significant correlations have been demonstrated between the average $\delta^{13}C$ values of local C3 plants and mean annual precipitations (Diefendorf et al., 2010; Kohn, 2010). Through differences in photosynthetic pathway and plant physiology, climate conditions act as a primary control on large-scale variation in $\delta^{13}C$ values of vegetation and on the distribution and abundance of C3 and C4 plants (Teeri and Stowe, 1976; Tieszen et al., 1997). Consequently, stable carbon isotope compositions of fossil guano reflect the stable isotope composition of plants, which are in turn related to local environmental conditions.

Furthermore, it is important to note that the mode of plantclimate interactions change over time, notably influenced by variations in atmospheric CO_2 concentration and $^{13}C/^{12}C$ ratios, i.e. Suess effect ($\delta^{13}C_{atm}$) (Arens et al., 2000; Prentice and Harrison, 2009). These modifications can produce important changes in plant $\delta^{13}C$ values, meaning that $\delta^{13}C$ values of past vegetation must be corrected from these parameters in order to quantify past environmental changes. A negative relationship between CO_2 concentrations and $\delta^{13}C$ values in plants has been documented by several authors (Van de Water et al., 1994; Feng and Epstein, 1995; Hatte et al., 2009). Indeed, CO_2 concentrations from the preindustrial period were lower than today, decreasing down to 200 ppm or less during the Last Glacial period (Barnola et al., 1987; Ahn and Brook, 2008). In addition, changes in $\delta^{13}C_{atm}$ have been shown to have a more direct effect than CO_2 concentration on plant $\delta^{13}C$ values (Farquhar et al., 1989; Feng and Epstein, 1995; Arens et al., 2000). The current $\delta^{13}C_{atm}$ value is close to 8.0‰ whereas the pre-industrial period was marked by $\delta^{13}C_{atm}$ estimated to be about 6.5‰ (Leuenberger et al., 1992; Keeling et al., 2005).

Consequently, $\delta^{13}C$ values of plants recorded in fossil guano must be corrected to take into account their development during periods with both different CO_2 concentrations and $\delta^{13}C_{atm}$. Firstly, we used CO_2 concentration values proposed by Ahn and Brook (2008) and we used a coefficient of 2.0 ± 0.1‰ per 100 ppm between CO_2 concentrations and plant $\delta^{13}C$ values, leading to obtain a maximal $\delta^{13}C$ correction of þ1.6‰ for the lowest CO_2 concentration of the Last Glacial Maximum. Secondly, we used data from Schmitt et al. (2012) who estimated $\delta^{13}C_{atm}$ variations ranging from 6.7 ± 0.06 to 6.3 ± 0.03‰ during the period spanning from 24 to 6 ka BP, with small variations ranging from 6.46 to 6.40 between 24.0 and 17.4 ka BP. Beyond 24.0 ka BP, the value used was 6.4‰. These two corrections have been calculated on the basis of the first sample (P13 e Suppl. material S2), which is characterized by a $\delta^{13}C_{atm}$ value of 6.6‰ and a CO_2 concentration of 265.4 ppm.

4. Results

Guano from modern Antillean fruit-eating bats collected from Blanchard Cave has a $\delta^{13}C$ value of 27.0‰ in contrast to those of fossil bat guano that range from 25.7 to 19.8‰ throughout the stratigraphic sequence (Table 2; Suppl. material S2; Fig. 5). These $\delta^{13}C$ values reflect a diet mainly based on C3 plants, which are associated for the highest values superior to 22‰, at least, with a contribution of C4 plants. Intra-level variations, which can be significant as in levels 5 and 12 with amplitudes in $\delta^{13}C$ variations reaching up to 5.1 and 5.9‰, respectively, are more important than the inter-level variations that do not exceed 3.1‰ (see levels 3, 5, 8, 10 and 12). Consequently, no correlation is evident between the various levels and climatic events, and then there is no reason to use the stratigraphic delimitations to fragment the isotopic signals, except to differentiate levels laminated from those non-laminated. The highest $\delta^{13}C$ values were observed in level 5 dated to the Bølling-Allerød interstadial and at the beginning of level 12 dated to around 34.7 ka BP, while the lowest $\delta^{13}C$ values were measured in the uppermost samples of the sequence associated with Younger-Dryas and the beginning of the Holocene. The $\delta^{13}C$ values corrected for CO_2 concentration and atmospheric $\delta^{13}C$ range from 25.7 to 18.8‰ (Fig. 5, dashed line). These corrections do not strongly

modify either the trends of $d^{13}C$ variations nor their intra-level magnitudes but shift the lower samples (dated to before the Lateglacial period) towards higher $d^{13}C$ values with a maximum offset of 1.6‰ in samples dated from Last Glacial Maximum, reinforcing contrasts between the isotopic compositions of present-day and past guano.

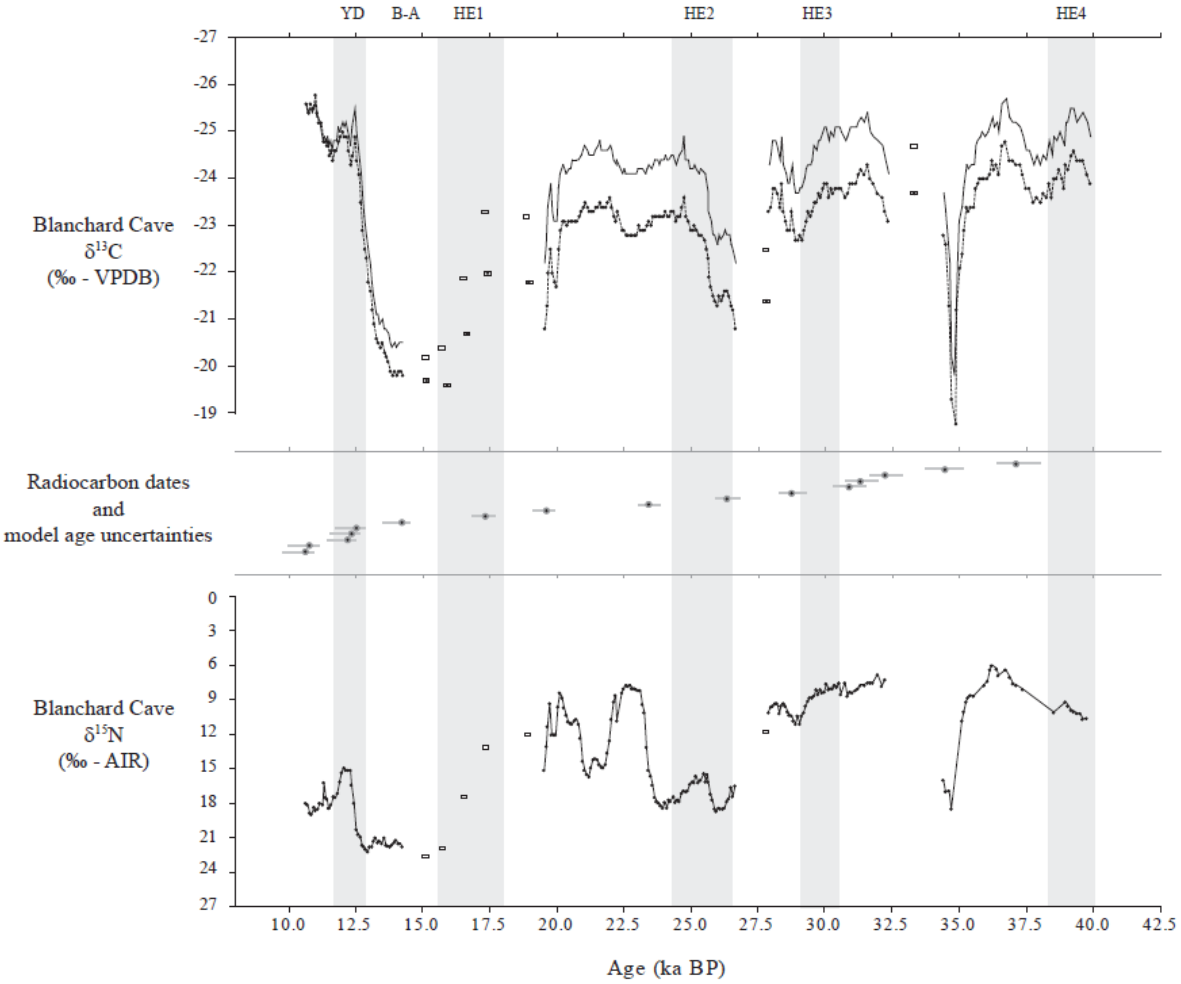

Fig. 5. Carbon and nitrogen isotope compositions of bat guano from Blanchard Cave and the corrected $d^{13}C$ values (dashed line) from CO_2 concentration and atmospheric $d^{13}C$ (see paragraph 3.4) reported along the age estimated from the age-depth model, illustrated with the age uncertainties calculated at 99.7% (Suppl. material S2).

Modern guano from Antillean fruit-eating bats has a $d^{15}N$ value of 11.1‰. Nitrogen isotope compositions of fossil bat guano range from 5.9 to 22.7‰ throughout the stratigraphic sequence, with a mean value of 13.5‰. Like carbon isotope compositions, the highest $d^{15}N$ values were observed in levels 5 and 6 that are dated to the Bølling-Allerød interstadial and Heinrich event 1, respectively. The lowest $d^{15}N$ values were measured in level 12 that has been dated to between 37 and 36 ka cal. BP. Furthermore, two sizable changes in $d^{15}N$, greater than 11‰ have been observed close to 23.5 and 35.0 ka cal. BP.

For the general trends, the d13C and d15N values are positively correlated throughout the sequence (Rho ¼ 0.43, $p < 0.0001$) except during level 8 (Rho ¼ 0.02, p ¼ 0.80). It is noteworthy that several time lags were not recorded in the same way by carbon and nitrogen isotope compositions of fossil guano. For example, during the Bølling-Allerød period, d13C values decreased from around 13.7 ka cal. BP, whereas d15N began to decrease around 12.9 ka cal. BP, at the beginning of the Younger-Dryas.

The C/N ratios vary from 3.3 to 6.0, which corresponds to the range of values for modern insectivorous bats (Bird et al., 2007; Emerson and Roark, 2007; Wurster et al., 2007) and close to that of modern frugivorous bats extending their diet to insects (Royer et al., 2015). These ratios measured in fossil guano from insectivorous bats are much higher than those that could be expected for altered samples because of oxidation and subsequent carbon release operating in tandem with nitrogen mineralization (Choa et al., 2016). C/N ratios are weakly, but significantly and negatively correlated with d13C (Rho ¼0.197, $p < 0.002$) and negatively correlated with d15N (Rho ¼0.503, $p < 0.0001$) throughout the sequence.

5. Discussion

5.1. Genesis of guano deposits and their preservation

The fossil bat guano deposit of Blanchard Cave indicates that bats regularly occupied the cave since the last 40 ka cal. BP, as evidenced by abundant fossil bat bones found throughout the deposit as well (Stoetzel et al., 2016). Eight bat species are currently known on Marie-Galante with four phytophageous, three insectivorous and one piscivorous bats (Masson et al., 1990; Breuil and Masson, 1991; McCarthy and Henderson, 1992). This modern fauna represents only a small part of the bat community inhabiting the Island during the Late Pleistocene, constituted at least by twelve species including four nectarivorous and frugivorous bats. No insect remains were recovered from the sequence, whereas the occurrence of degraded vegetal tissues in the sediment suggests that the Pleistocene guano in the cave mostly resulted from phytophageous bats. On the other side, consumption of insects cannot be excluded, both considering the occurrence of insectivorous bat remains in the deposit, and the C/N ratio closer to bats including at least a part of insects in their diet compared to those having a restricted frugivorous diet (Royer et al., 2015). This part of insect consumption is difficult to quantify. Even if this issue does not compromise the data or interpretations, as $\delta^{13}C$ values of both reflect plant values and therefore humidity, the main risk is to add uncertainties of one trophic level in case where bat populations are switching from one dominant guild to another one. However, the absence of sizable variations in C/N ratios and in mineralogical contents throughout the deposit of Blanchard Cave let to suggest that no major changes have occurred in bat occupations of the cave in term of guild proportion. Consequently, stable isotope compositions of this fossil guano should mainly reflect the composition of plants consumed by these individuals.

As noted above, the massive sedimentary structure associated with burrow imprints in levels 6, 7, 9 and 11 provide clear evidence for bioturbation of a still unclear nature, although the action of ground dweller animals, such as the burrowing owl (Athene cunicularia), which is known to have inhabited the Caribbean islands during the Pleistocene (Pregill and Olson, 1981; Pregill et al., 1994) is likely. Apart from these levels, the other deposits are characterized by well-preserved laminated sediments with no evidence for bioturbation or post-depositional reworking. Moreover, observation of thin sections did not reveal the presence of either an organic mobile fraction in the sediment or patterns of water percolation. Finally, the dry micro-climate of Blanchard Cave (Lenoble et al., 2015) has also favored the preservation of buried organic matter. All these criteria suggest that the stable isotope compositions of laminated fossil guano are likely to reliably record changes in local vegetation patterns in response to global climatic forcing.

In particular, the preservation of the original $\delta^{15}N$ signal is regularly questioned through studies dealing with fossil guano, due to potential post-depositional alteration involving volatilization of ammonia. Such alterations, even if they seem to not engender significant carbon isotope fractionation, may favor ^{15}N-enrichment by as much as 7‰ (Mizutani and Wada, 1988; Bird et al., 2007; Wurster et al., 2010b). Two patterns in $\delta^{15}N$ values are considered as suspicious: firstly, fossil guano values higher

than modern ones, even if such values can result equally from other parameters such as aridity; and secondly, the chemical changes should invariably lead to strong correlations between elemental ratios and isotopic compositions (Wurster et al., 2010b). In this study, the Blanchard Cave is characterized by a large range of $\delta^{15}N$ values, with $\delta^{15}N$ values higher than modern ones by about 10‰, and that co-vary with C/N ratios throughout the sequence. As a consequence, variations in $\delta^{15}N$ values observed at Blanchard Cave are difficult to interpret. Indeed, feces nitrogen directly reflects the nitrogen isotope composition of the diet, therefore significant changes in bat diet could explain these changes in $\delta^{15}N$ values. A second possibility concerns the impacts of significant changes in plant communities, with modifications of leguminous plant proportions (leading to $\delta^{15}N$ values close to zero when these plants are abundant) or with changes of nitrogen sources used by plants (ammonium NH_4 versus nitrate NO_3). It is noticeable that during some intervals, such as the Allerød, changes in $\delta^{13}C$ values preceded those observed for the $\delta^{15}N$ values by 500–2000 years. Similar time lags between climatic changes and $\delta^{15}N$ records of fauna have equally been documented in Europe during the Late Pleistocene, probably due to the complexity of the soil-plant nitrogen cycle (e.g. Stevens et al., 2008; Stevens et al., 2014). Finally, these significant changes in $\delta^{13}C$ values, which partly co-varied with $\delta^{15}N$ values considering a slight time lag, could suggest a record of similar environmental conditions changes.

As the organic matter has undergone considerable decomposition and loss through microbial reprocessing and remineralisation, it is important to assess the potential impact of post-depositional processes on the isotopic composition of guano. Although diagenetic influences cannot be completely ruled out, both the lack of significant covariation between elemental ratios and carbon isotope values and the lack of significant differences between elemental ratios and age attest a lack of significant diagenetic alteration at least for carbon.

5.2. Environmental conditions on Marie-Galante from 40 to 10 ka BP

The Blanchard Cave record indicates that environmental conditions from 40 to 10 ka cal. BP were locally drier than today because bat guano $\delta^{13}C$ values are higher than the modern ones (Fig. 6). Meanwhile, over the period spanning from 40 to 19 ka cal. BP, guano $\delta^{13}C$ values tend to be low, suggesting overall wetter environmental conditions compared with 16 - 13 ka cal. BP. The relatively high $\delta^{13}C$ values suggest four dry events. The first one is a brief dry period of about 500 years, which peaked at 34.7 ka cal. BP and was also characterized by an increase in $\delta^{15}N$ values. This dry event, which is one of the biggest and shortest through the Blanchard record, has no equivalent with records from other proxies (Fig. 6). A second dry event occurred from 27.8 to 26 ka cal. BP. Dry conditions returned around 19.5 ka cal. BP and then again between Heinrich event 1 and the Bølling interstadial, with the period from 16.6 to 13.5 ka cal. BP characterized by the lowest $\delta^{13}C$ values and highest $\delta^{15}N$ values. The timing of the onset of this last drought event is, however, not accurately documented due to the bioturbated nature of levels 7 and 6. Nevertheless, this dry period continued until at least the Allerød interstadial, when $\delta^{13}C$ values began to progressively decrease. Samples from the final level 3, which are estimated to date between the Younger-Dryas and the beginning of the Holocene based on age uncertainties in the agedepth model, recorded the lowest bat guano $\delta^{13}C$ values suggesting wetter conditions without reaching those prevailing today (Fig. 6). However, it is noteworthy that Younger-Dryas could have been blurred by the roof collapse associated with level 4. Indeed, we cannot exclude that this event may have resulted in a lag in the record in the time span between 12.6 and 11.5 ka cal. BP following uncertainties from the model-age.

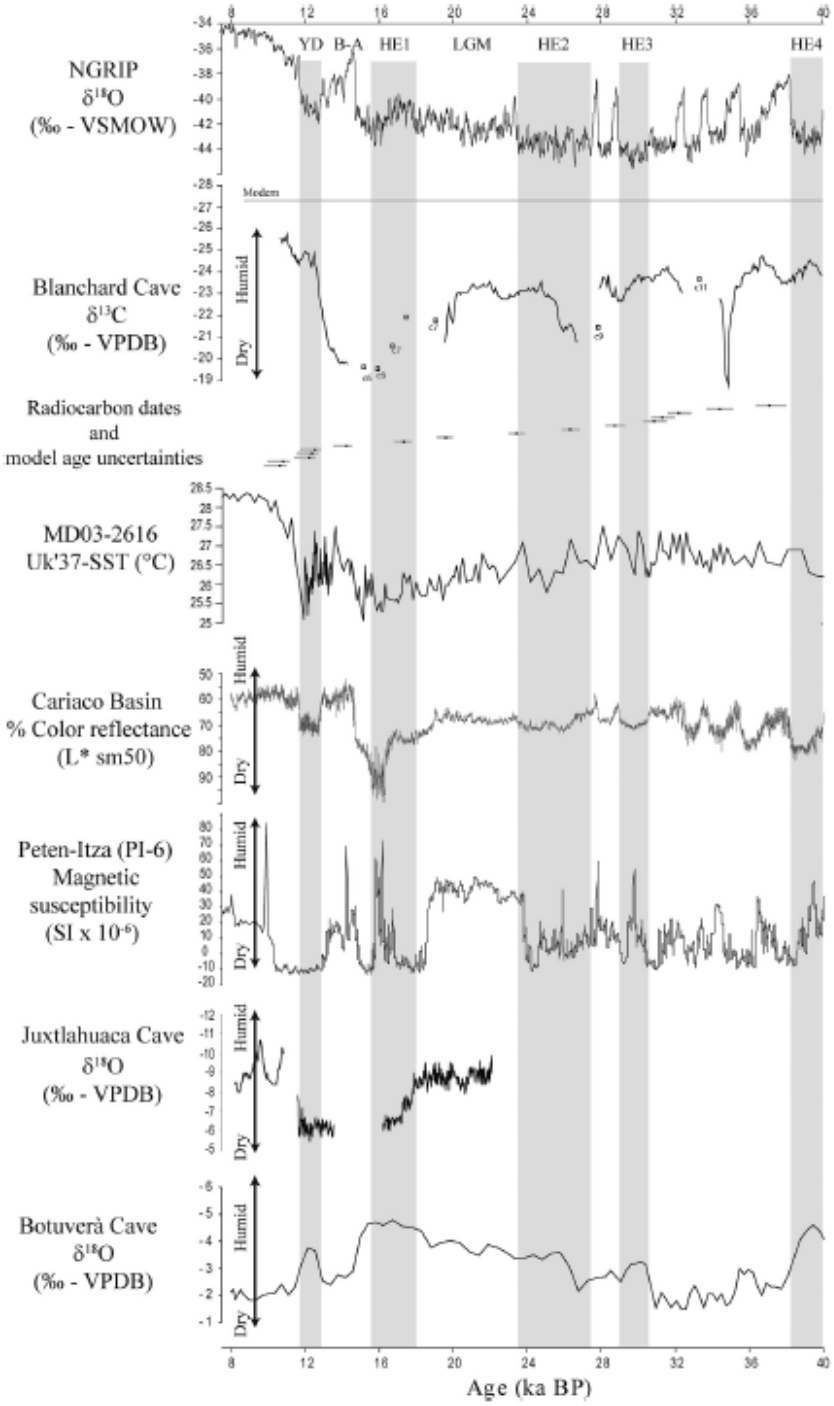

Fig. 6. Comparison between NGRIP d^{18}O ice records from Greenland (North Greenland Ice Core Project, 2004); Carbon and nitrogen isotope compositions of bat guano from Blanchard Cave reported along the geological age of samples estimated from the age-depth model. For the Blanchard Cave, the black line corresponds to corrected d^{13}C values from CO_2 concentration and atmospheric d^{13}C (see paragraph 3.4). Stable isotope values of guano sampled from bioturbated levels are illustrated by a square. Present-day carbon isotope compositions of guano corrected from CO_2 concentration and atmospheric d^{13}C are illustrated by two lines. Samples of guano used for radiocarbon dates are reported with age uncertainties obtained from the age-depth model; NGRIP d^{18}O ice records from Greenland (North Greenland Ice Core Project, 2004); Uk'37-SST (C) measurements in core MD032616 (Rama-Corredor et al., 2015); Percentage of color reflectance (L* sm50) from the Cariaco Basin (Deplazes et al., 2013); Magnetic susceptibility measured in samples coming from Peten Itz a core 6 (PI-6) (Escobar et al., 2012); Oxygen isotope compositions measured from Juxtlahuaca Cave (Lachniet et al., 2013); and oxygen isotope compositions measured from Botuvera Cave (Wang et al., 2007). Abbreviations are: YD ¼ Younger-Dryas event; HE ¼ Heinrich event; B-A ¼ Bølling e Allerød events; LGM ¼ Last Glacial Maximum. Grey intervals indicate the four Heinrich and the Younger Dryas events.

5.3. Climatic and environmental conditions of the Caribbean area

The Late Pleistocene of the Caribbean Basin has been considered for a long time as a uniformly dry period, mainly due to the scarcity of continental archives such as speleothems or lacustrine deposits, extending beyond the dry period of the Younger-Dryas (Goodfriend and Mitterer, 1988; Hodell et al., 1991; Leyden, 1995; HigueraGundy et al., 1999). In the Eastern Caribbean Islands, one of the rare Pleistocene sedimentary deposits comes from the 'Wallywash Great Pond' in Jamaica. The period spanning from 93.0 to 9.5 ka BP, however, was roughly described as dominated by dry and cold conditions (Street-Perrott et al., 1993; Holmes, 1998), an interpretation fitting the common model of a succession of wet interglacial and dry glacial stages prevailing in neotropical regions.
The few currently known sedimentary continuous records that extended beyond the Late Glacial period have challenged this 'wetdry' dichotomy, notably that from the Cariaco Basin, Venezuela (Peterson et al., 2000; Haug et al., 2001; Gonzalez et al., 2008; Deplazes et al., 2013) and the Lake Peten Itz a, Guatemala (Hodell et al., 2008; Perez et al., 2011; Escobar et al., 2012). These two sedimentary archives have shown, as observed under high latitude regions, the presence of a considerable tropical climate variability in the Caribbean Basin, as now equally observed in the Blanchard Cave sequence. The development of humid or dry climatic conditions has been interpreted as resulting from modifications of the mean position of the ITCZ (Fig. 6). In particular, studies of the Peten Itza deposits revealed that the western Caribbean area witnessed cooler climate conditions (2.5 C) during the Last Glacial Maximum (23e18 ka BP) compared to current conditions (Hodell et al., 2008), decreasing during Heinrich Stadial by up 6e10 C relative to today (Grauel et al., 2016). In addition, the Last Glacial Maximum was more humid than the one spanning from ~19 to 15 ka BP (Heinrich event 1) (Fig. 6), which is considered to have experienced the most arid conditions based on ostracod oxygen stable isotope compositions (Escobar et al., 2012). Stable isotope compositions of bat guano accumulated in the Blanchard Cave generally reflect overall drier environmental conditions during the Late Pleistocene compared to modern ones, supporting the hypothesis of arid conditions connected to the strengthening of trade winds. Moreover, stable isotope compositions of guano from the Blanchard Cave, the first terrestrial sequence documenting Marine Isotopic Stages 3 and 2 in the Lesser Antilles, suggest that the Last Glacial Maximum period in this area was characterized by relative humid conditions in comparison to Heinrich event 1 (Fig. 6). Similar patterns have been observed at Peten Itz a and in stalagmites in southwestern Mexico from Juxtlahuaca Cave (Lachniet et al., 2013), which present low $\delta^{18}O$ values of calcite during the Last Glacial Maximum period. Climate proxies from South America present an inverse pattern due to ITCZ migration, as illustrated by speleothems from Botuvera Cave in Brazil that show a drier LGM compared to the Heinrich event 1 (Wang et al., 2007).

However, the environmental variations observed at Blanchard Cave do not perfectly match patterns recognized in the Cariaco Basin or at Peten Itz a and Botuver a Cave (Brazil). In particular, an opposite trend seems to be identified for the Younger-Dryas and to a lesser extent for Heinrich event 2. In fact, the pollen signal from Peten Itz a indicates that the period of maximum aridity spanned from ~18 to 11 ka BP (including Heinrich event 1 and the YoungerDryas), despite sufficiently wet conditions during the YoungerDryas that could support a forest cover with a gradual change toward more mesic conditions from 13 to 11 ka BP (Bush et al., 2009). The Juxtlahuaca Cave stalagmites present a similar climatic record with high $\delta^{18}O$ values recorded throughout Heinrich event 1 to the end of the Younger-Dryas (Lachniet et al., 2013), again suggesting this period was especially dry. Such discrepancies is relatively surprising. Thus, they questioned the reliability of ITCZ model in this area that can be in reality more complex than previously known, for example by experiencing a regionalization of climate in response to interrelated atmospheric conditions, as already evidenced during the mid-Holocene in northern

Caribbean (e.g. Malaize et al., 2011). To investigate such issues, complementary records are, however, necessary. On the other side, these discrepancies questioned also the effects of uncertainties in each model age from the different proxies used, which can be due to different tuning models or to different radiocarbon date calibrations. Nonetheless, when considering the different uncertainties in each age model, the different records can be reconciled. Indeed, dry conditions prevailing during the Younger-Dryas could be observed in the Blanchard Cave record if the errors on the age model are taken into account (Fig. 6). Similarly, the weak amount of age control points around the Heinrich event 2 do not allow us to conclude that Blanchard Cave record differs from other Caribbean and South American records. Heinrich events 1, 3 and 4 are relatively consistent between records. When more arid conditions are observed at Blanchard Cave, Cariaco Basin and Peten Itz a, more humid conditions are experienced at Botuvera cave (Fig. 6). This suggests that the Blanchard Cave record is a robust proxy of past ITCZ migration.

The ITCZ migration is driven by changes in the hemispheric temperature gradients. During abrupt events associated to HEs, the reduction of the AMOC (Bard et al., 2000) affected the displacement of the ITCZ southward, reinforcing trade wind and increasing both the temperature and salinity of the tropical Atlantic surface waters due to a reduced marine heat export northward (Chiang et al., 2002; Donders et al., 2011; Arbuszewski et al., 2013; Came et al., 2013). Since many years, teleconnections between polar and tropical latitudes have been investigated (e.g. Peterson et al., 2000; Deplazes et al., 2013), questioning the role played by millennial variations in North Atlantic climate on climate from lower latitudes. Recently, Rama-Corredor et al. (2015) have showed that Uk'37-SST (C) measurements from MD03-2616 core, located in Guiana Basin, covaried with the temperature changes observed in Greenland during interglacial periods. On a contrary, they showed a lack of synchrony during glacial periods, suggesting an Arcticetropical decoupling when a substantial reduction in the AMOC takes place. MD03-2616 is located in the confluence of Northern (NEC) and Southern Hemisphere waters (NBC, SEC) suggesting a stronger influence of southern Hemisphere waters during glacial periods. When comparing with another tropical region, it is remarkable that variations in carbon isotope compositions from the Blanchard Cave are relatively similar to those observed in a Bromine (Br) stack obtained by XRF counts from six sedimentary marine sediment cores located in the Arabian Sea (Fig. 7) (Caley et al., 2013). Brominated organic compounds in marine sediments are connected to primary producers (macroalgae) and heterotrophic organisms, with variations in the Bromine counts considered as proxies of marine organic carbon (productivity) changes (Ziegler et al., 2008). Caley et al. (2013) suggested that the Bromine stack could be related to the Indian monsoon. The India monsoon and associated position of the ITCZ reflect a bi-polar influence with a Southern Hemisphere imprint during the glacial period and a more significant role of the Northern Hemisphere during the last deglaciation. Consequently, the close pattern observed between the carbon isotope compositions from the continental archive of the Blanchard Cave and Arabian Sea records could suggest that the Eastern Caribbean islands were also under the influence of bipolar temperature gradients that impacted the mean location of the ITCZ. Hodell et al. (2008) have already indicated that dry periods in Peten Itza were generally associated with warmings in Antarctica (AIM) during MIS 3. A Southern Hemisphere imprint could be visible during the glacial period as suggested by the relative close agreement (considering model age uncertainties) between Blanchard Cave records and the ice core Antarctica record of EDML (Fig. 7). The significant abrupt variability observed in the Blanchard record therefore reflects past migration of the ITCZ driven by bipolar temperature gradients, a mechanism that also contributed to the ITCZ migration in west Africa (Weldeab, 2012) and Arabian sea.

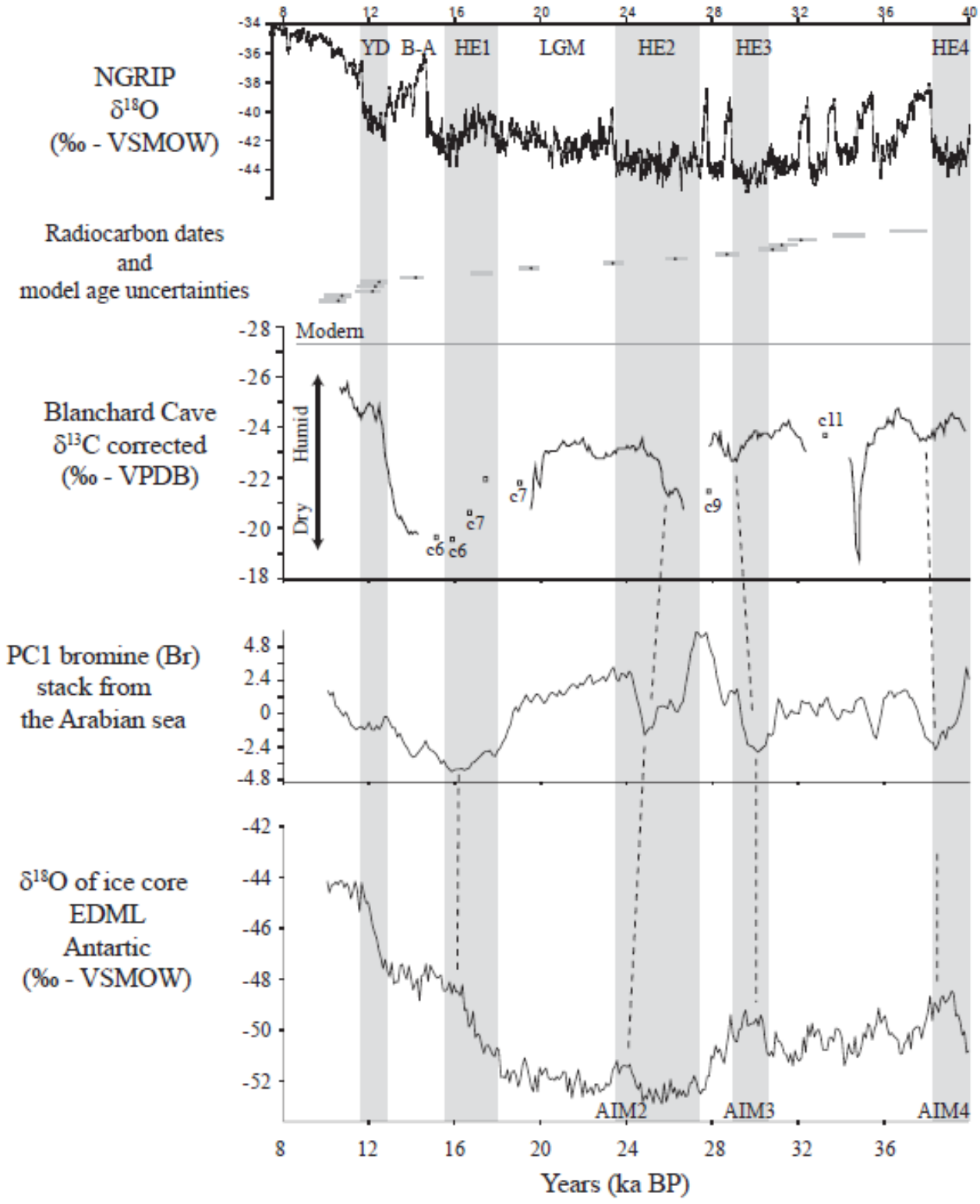

Fig. 7. Comparison between A) NGRIP $d^{18}O$ ice records from Greenland (North Greenland Ice Core Project, 2004); B) The $d^{13}C$ values from the Blanchard Cave corrected from CO_2 concentration and atmospheric $d^{13}C$ (see paragraph 3.4). C) The PC1 Bromine stack from marine cores located in the Arabian Sea (Caley et al., 2013). D) Antarctic $d^{18}O$ of ice core EDML Dome C. AIM ¼ Antarctic Isotope Maximum.

6. Conclusions

Fossil bat guano has been accumulated between 40 and 10 ka cal. BP in Blanchard Cave located on the island of Marie-Galante in the Eastern Caribbean. Carbon and nitrogen isotope compositions of this guano revealed this tropical region to have experienced overall drier, and above all, more variable environmental conditions during this period compared to present-days. More specifically, variations in the isotopic compositions of bat guano are here interpreted to reflect major changes in the Late Pleistocene vegetation. Relatively wet environmental conditions prevailed during the second part of MIS 3 and the beginning of MIS 2, even still drier than those of Holocene, while the final part of the LGM and the very beginning of the Late Glacial regionally form an arid maximum during a two to three millennium period from ca 16 to 13 ka cal. BP. When considering uncertainties in the model age, the isotopic record of Blanchard Cave are relatively similar to those observed with known records from Caribbean and South American records, suggesting that abrupt variability observed in the Blanchard record therefore reflect past migration of the ITCZ. The similar pattern equally observed between Blanchard Cave record and Arabian sea records suggests that islands of the eastern Caribbean Basin were also under the influence of bipolar temperature gradients that impacted the mean location of the ITCZ with a Southern Hemisphere imprint during the glacial period and a more significant role of the Northern Hemisphere during the last deglaciation.

Acknowledgments

This study was conducted as a part of the CNRS BIVAAG Program with support from a European PO-FEDER grant 2007-2013 n2/ 2.4/-33456, the Guadeloupe Regional Council, the DEAL of Guadeloupe, and the DAC of Guadeloupe. This is Past4Future contribution and the research presented here received funding from the European Union's Seventh Framework programme (FP7/ 2007-2013) under grant agreement nº 243908, "Past4Future. Climate change - Learning from the past climate". The authors would also like to thank P. Martinez, C. Hatte, S. Desprat, V. Han- quiez, E. Puech, M. Corbe and B. Gravina for their help. The authors would like to thank anonymous reviewers for their constructive remarks and improvements of the manuscript.

References

Ahn, J., Brook, E.J., 2008. Atmospheric CO_2 and climate on millennial time scales during the last glacial period. Science 322, 83e85.

Amundson, R., Austin, A.T., Schuur, E.A.G., Yoo, K., Matzek, V., Kendall, C., Uebersax, A., Brenner, D., Baisden, W.T., 2003. Global patterns of the isotopic composition of soil and plant nitrogen. Glob. Biogeochem. Cycle 17, 1031. http:// dx.doi.org/10.1029/2002GB001903.

Arbuszewski, J.A., deMenocal, P.B., Cleroux, C., Bradtmiller, L., Mix, A., 2013. Meridional shifts of the Atlantic intertropical convergence zone since the Last Glacial Maximum. Nat. Geosci. 6, 959e962.

Arens, N.C., Jahren, A.H., Amundson, R., 2000. Can C3 plants faithfully record the carbon isotopic composition of atmospheric carbon dioxide? Paleobiology 26, 137e164.

Bailon, S., Bochaton, C., Lenoble, A., 2015. New data on Pleistocene and Holocene herpetofauna of Marie Galante (Blanchard Cave, Guadeloupe Islands, French West Indies): insular faunal turnover and human impact. Quat. Sci. Rev. 128, 127e137.

Barbotin, M., 1987. Archeologie antillaise: Arawaks et Caraïbes. Parc naturel de Guadeloupe.

Bard, E., Rostek, F., Turon, J.-L., Gendreau, S., 2000. Hydrological impact of Heinrich events in the subtropical northeast Atlantic. Science 289, 1321e1324.

Barnola, J.M., Raynaud, D., Korotkevich, Y.S., Lorius, C., 1987. Vostok ice core provides 160,000-year record of atmospheric CO_2. Nature 329, 408e414.

Beets, C.J., Troelstra, S.R., Grootes, P.M., Nadeau, M.J., Borg, K.V., de Jong, A.F.M., Hofman, C.L., Hoogland, M.L.P., 2006. Climate and pre-Columbian settlement at Anse a la Gourde, Guadeloupe, Northeastern Caribbean. Geoarchaeology 21, 271e280.

Bender, M.M., 1971. Variation in the $^{13}C/^{12}C$ ratios of plants in relation to the pathway of photosynthetic carbon dioxide fixation. Phytochem 10, 1234e1244. Bertran, P., Bonnissent, D., Imbert, D., Lozouet, P., Serrand, N., Stouvenot, C., 2004. Paleoclimat des Petites Antilles depuis 4000 ans BP: l'enregistrement de la lagune de Grand-Case a Saint-Martin. C. R. Geosci. 336, 1501e1510.

Bird, M.I., Boobyer, E.M., Bryant, C., Lewis, H.A., Paz, V., Stephens, W.E., 2007. A long record of environmental change from bat guano deposits in Makangit Cave, Palawan, Philippines. Earth Environ. Sci. T. Roy. Soc. Edinb. 98, 59e69.

Blaauw, M., 2010. Methods and code for 'classical'age-modelling of radiocarbon sequences. Quat. Geochronol. 5, 512e518.

Blunier, T., Brook, E.J., 2001. Timing of millennial-scale climate change in Antarctica and Greenland during the last glacial period. Science 291, 109e112.

Bochaton, C., Grouard, S., Cornette, R., Ineich, I., Lenoble, A., Tresset, A., Bailon, S., 2015. Fossil and subfossil herpetofauna from cadet 2 cave (Marie-Galante, Guadeloupe Islands, F. W. I.): evolution of an insular herpetofauna since the Late Pleistocene. C. R. Palevol 14, 101e110.

Bond, G., Broecker, W., Johnsen, S., McManus, J., Labeyrie, L., Jouzel, J., Bonani, G., 1993. Correlations between climate records from North Atlantic sediments and Greenland ice. Nature 365, 143e147.

Bond, R.M., Seaman, G.A., 1958. Notes on a colony of Brachyphylla cavernarum. J. Mammal. 39, 150e151.

Bouysse, P., Garrabe, F., Mauboussin, T., Andreieff, P., Batistini, R., Carlier, P., Hinschberger, F., Rodet, J., 1993. Carte geologique departement de la Guadeloupe. BRGM, Orleans.

Breuil, M., Masson, D., 1991. Quelques remarques sur la biogeographie des chauvessouris des Petites Antilles. C. R. Soc. Biogeogr. 67, 25e39.

Broccoli, A.J., Dahl, K.A., Stouffer, R.J., 2006. Response of the ITCZ to Northern Hemisphere cooling. Geophys. Res. Lett. 33, L01702.

Bush, M., Correa-metrio, A., Hodell, D., Brenner, M., Anselmetti, F., Ariztegui, D., Mueller, A., Curtis, J., Grzesik, D., Burton, C., Gilli, A., 2009. Re-evaluation of climate change in lowland Central America during the last glacial maximum using new sediment cores from Lake Peten Itza, Guatemala. In: Vimeux, F., Sylvestre, F., Khodri, M. (Eds.), Past Climate Variability in South America and Surrounding Regions. Springer Netherlands, pp. 113e128.

Caley, T., Zaragosi, S., Bourget, J., Martinez, P., Malaize, B., Eynaud, F., Rossignol, L., Garlan, T., Ellouz-Zimmermann, N., 2013. Southern Hemisphere imprint for Indo-Asian summer monsoons during the last glacial period as revealed by Arabian Sea productivity records. Biogeosciences 10, 7347e7359.

Came, R.E., Curry, W.B., Oppo, D.W., Broccoli, A.J., Stouffer, R.J., Lynch-Stieglitz, J., 2013. North Atlantic Intermediate Depth Variability during the Younger Dryas: Evidence from Benthic Foraminiferal Mg/Ca and the Gfdl R30 Coupled Climate Model, Ocean Circulation: Mechanisms and Impacts - Past and Future Changes of Meridional Overturning. American Geophysical Union, pp. 247e263.

Charles, C.D., Lynch-Stieglitz, J., Ninnemann, U.S., Fairbanks, R.G., 1996. Climate connections between the hemisphere revealed by deep sea sediment core/ice core correlations. Earth Planet. Sci. Lett. 142, 19e27.

Chiang, J.C.H., Kushnir, Y., Giannini, A., 2002. Deconstructing Atlantic Intertropical Convergence Zone variability: influence of the local cross-equatorial sea surface temperature gradient and remote forcing from the eastern equatorial Pacific. J. Geophys. Res. Atmos. 107. ACL 3-1-ACL 3e19.

Choa, O., Lebon, M., Gallet, X., Dizon, E., Ronquillo, W., Jago-on, S.C., Detroit, F., Falgueres, C., Ghaleb, B., S emah, F., 2016. Stable isotopes in guano: potential contributions towards

palaeoenvironmental reconstruction in Tabon Cave, Palawan, Philipinnes. Quat. Int. 416 27e37. http://dx.doi.org/10.1016/ j.quaint.2015.12.034.
Cleary, D.M., Onac, B.P., Forray, F.L., Wynn, J.G., 2016. Effect of diet, anthropogenic activity, and climate on $\delta^{15}N$ values of cave bat guano. Palaeogeo. Paleoclim. Paleoecol. 461, 87e97.
Curtis, J.H., Hodell, D.A., 1993. An isotopic and trace element study of ostracods from Lake Miragoane, Haiti: a 10,500 year record of paleosalinity and paleotemperature changes in the Caribbean. In: Swart, P.K., Lohmann, K.C., Mckenzie, J., Savin, S. (Eds.), Climate Change in Continental Isotopic Records. American Geophysical Union, pp. 135e152.
Dansgaard, W., Johnsen, S.J., Clausen, H.B., Dahl-Jensen, D., Gundestrup, N., Hammer, C.U., Hvidberg, C.S., Steffensen, J.P., Sveinbjornsdottir, A.E., Jouzel, J., Bond, G., 1993. Evidence for general instability of past climate from a 250-kyr ice-core record. Nature 364, 218e220.
Deplazes, G., Lückge, A., Peterson, L.C., Timmermann, A., Hamann, Y., Hughen, K.A., Ro€hl, U., Laj, C., Cane, M.A., Sigman, D.M., Haug, G.H., 2013. Links between tropical rainfall and North Atlantic climate during the last glacial period. Nat. Geosci. 6, 213e217.
De Niro, M.J., Epstein, S., 1981. Influence of diet on the distribution of nitrogen isotopes in animals. Geochim. Cosmochim. Acta 45, 341e351.
Des Marais, D.J., Mitchell, J.M., Meinschein, W.G., Hayes, J.M., 1980. The carbon isotope biogeochemistry of the individual hydrocarbons in bat guano and the ecology of the insectivorous bats in the region of Carlsbad, New Mexico.
Geochim. Cosmochim. Acta 44, 2075e2086.
Diefendorf, A.F., Mueller, K.E., Wing, S.L., Koch, P.L., Freeman, K.H., 2010. Global patterns in leaf ^{13}C discrimination and implications for studies of past and future climate. PNAS 107, 5738e5743.
Donders, T., de Boer, H., Finsinger, W., Grimm, E., Dekker, S., Reichart, G., WagnerCremer, F., 2011. Impact of the Atlantic Warm Pool on precipitation and temperature in Florida during North Atlantic cold spells. Clim. Dyn. 36, 109e118.
Ehleringer, J.R., Cerling, T.E., Helliker, B.R., 1997. C4 photosynthesis, atmospheric CO_2, and climate. Oecologia 112, 285e299.
Emerson, J.K., Roark, A.M., 2007. Composition of guano produced by frugivorous, sanguivorous, and insectivorous bats. Acta Chiropterol. 9, 261e267.
Escobar, J., Hodell, D.A., Brenner, M., Curtis, J.H., Gilli, A., Mueller, A.D., Anselmetti, F.S., Ariztegui, D., Grzesik, D.A., Perez, L., Schwalb, A., Guilderson, T.P., 2012. A ~43-ka record of paleoenvironmental change in the Central American lowlands inferred from stable isotopes of lacustrine ostracods. Quat. Sci. Rev. 37, 92e104.
Farquhar, G.D., Ehleringer, J.R., Hubick, K.T., 1989. Carbon isotope discrimination and photosynthesis. Annu. Rev. Plant Biol. 40, 503e537.
Feng, X.H., Epstein, S., 1995. Carbon isotopes of trees from arid environments and implications for reconstructing atmospheric CO_2 concentration. Geochim. Cosmochim. Acta 59, 2599e2608.
Fensterer, C., Scholz, D., Hoffmann, D.L., Spo€tl, C., Schro€der-Ritzrau, A., Horn, C., Pajon, J.M., Mangini, A., 2013. Millennial-scale climate variability during the last 12.5 ka recorded in a Caribbean speleothem. Earth Planet. Sci. Lett. 361, 143e151.
Forray, F.L., Onac, B.P., Tantau, B., Wynn, J.G., Tamas, T., Coroiu, I., Giurgiu, A., 2015. A Late Holocene environmental history of a bat guano deposit from Romania: an isotopic and pollen study. Quat. Sci. Rev. 127, 141e154. http://dx.doi.org/ 10.1016/j.quascirev.2015.05.022.
Gala, M., Lenoble, A., 2015. Evidence of the former existence of an endemic macaw in Guadeloupe, Lesser Antilles. J. Ornithol. 156, 1061e1066.
Gamble, D.W., Curtis, S., 2008. Caribbean precipitation: review, model and prospect. Prog. Phys. Geogr. 32, 265e276.
Gamble, D.W., Parnell, D.B., Curtis, S., 2008. Spatial variability of the Caribbean midsummer drought and relation to north Atlantic high circulation. Int. J. Climatol. 28, 343e350.

Gazquez, F., Calaforra, J.M., Stoll, H., Sanna, L., Forti, P., Lauritzen, S.E., Delgado, A., Rull, F., Martínez-Frías, J., 2013. Isotope and trace element evolution of the Naica aquifer (Chihuahua, Mexico) over the past 60,000 yr revealed by speleothems. Quat. Res. 80, 510e521.
Giannini, A., Cane, M.A., Kushnir, Y., 2001. Interdecadal changes in the ENSO teleconnection to the Caribbean Region and the North Atlantic Oscillation. J. Clim. 14, 2867e2879.
Giannini, A., Kushnir, Y., Cane, M.A., 2000. Interannual variability of Caribbean rainfall, ENSO, and the Atlantic Ocean. J. Clim. 13, 297e311.
Gonzalez, C., Dupont, L.M., Behling, H., Wefer, G., 2008. Neotropical vegetation response to rapid climate changes during the last glacial period: palynological evidence from the Cariaco Basin. Quat. Res. 69, 217e230.
Goodfriend, G.A., Mitterer, R.M., 1988. Late quaternary land snails from the north coast of Jamaica: local extinctions and climatic change. Palaeogeo. Paleoclim. Paleoecol. 63, 293e311.
Grauel, A.L., Hodell, D.A., Bernasconi, S.M., 2016. Quantitative estimates of tropical temperature change in lowland Central America during the last 42 ka. Earth Planet. Sci. Lett. 438, 37e46.
Grouard, S., Bonnissent, D., Courtaud, P., Fouere, P., Lenoble, A., Richard, G., Romon, T., Serrand, N., Stouvenot, C., 2013. Frequentation amerindienne des cavites des Petites Antilles. In: 24e Congres de l'asociation internationale des Archeologues de la caraïbe, pp. 277e295.
Handley, L.L., Austin, A.T., Stewart, G.R., Robinson, D., Scrimgeour, C.M., Raven, J.A., Schmidt, S., 1999. The ^{15}N natural abundance ($d^{15}N$) of ecosystem samples reflects measures of water availability. Funct. Plant Biol. 26, 185e199.
Hatte, C., Rousseau, D.D., Guiot, J., 2009. Climate reconstruction from pollen and $d^{13}C$ records using inverse vegetation modeling - implication for past and future climates. Clim. Past. 5, 147e156.
Haug, G.H., Hughen, K.A., Sigman, D.M., Peterson, L.C., Ro€hl, U., 2001. Southward migration of the intertropical convergence zone through the Holocene. Science 293, 1304e1308.
Herrera, L.G., Gerardo, L., Hobson, K.A., Manzo, A., Estrada, B., Sanchez-Cordero, V., Mendez, C., 2001a. The role of fruits and insects in the nutrition of frugivorous bats: evaluating the use of stable isotope models 1. Biotropica 33, 520e528.
Herrera, L.G., Hobson, K.A., Leticia, M.M., Ramírez, P.N., Mendez, C.G., SanchezCordero, V., 2001b. Sources of protein in two species of phytophagous bats in a seasonal dry forest: evidence from stable-isotope analysis. J. Mammal. 82, 352e361.
Higuera-Gundy, A., Brenner, M., Hodell, D.A., Curtis, J.H., Leyden, B.W., Binford, M.W., 1999. A 10,300 ^{14}C yr record of climate and vegetation change from Haiti. Quat. Res. 52, 159e170.
Hodell, D.A., Anselmetti, F.S., Ariztegui, D., Brenner, M., Curtis, J.H., Gilli, A., Grzesik, D.A., Guilderson, T.J., Müller, A.D., Bush, M.B., 2008. An 85-ka record of climate change in lowland Central America. Quat. Sci. Rev. 27, 1152e1165.
Hodell, D.A., Curtis, J.H., Jones, G.A., Higuera-Gundy, A., Brenner, M., Binford, M.W., Dorsey, K.T., 1991. Reconstruction of Caribbean climate change over the past 10,500 years. Nature 352, 790e793.
Holmes, J.A., 1998. A late Quaternary ostracod record from Wallywash Great Pond, a Jamaican marl lake. J. Paleolimnol. 19, 115e128.
Keeling, C.D., Piper, S.C., Bacastow, R.B., Wahlen, M., Whorf, T.P., Heimann, M., Meijer, H.A., 2005. Atmospheric CO_2 and $^{13}CO_2$ Exchange with the Terrestrial
Biosphere and Oceans from 1978 to 2000: Observations and Carbon Cycle Implications, a History of Atmospheric CO_2 and its Effects on Plants, Animals, and Ecosystems. Springer, pp. 83e113.
Kelly, J.F., 2000. Stable isotopes of carbon and nitrogen in the study of avian and mammalian trophic ecology. Can. J. Zool. 78, 1e27.
Kohn, M.J., 2010. Carbon isotope compositions of terrestrial C3 plants as indicators of (paleo)ecology and (paleo)climate. PNAS 107, 19691e19695.

Kolb, K.J., Evans, R.D., 2002. Implications of leaf nitrogen recycling on the nitrogen isotope composition of deciduous plant tissues. New Phytol. 156, 57e64.
Lachniet, M.S., Asmerom, Y., Burns, S.J., Patterson, W.P., Polyak, V.J., Seltzer, G.O., 2004. Tropical response to the 8200 yr BP cold event? Speleothem isotopes indicate a weakened early Holocene monsoon in Costa Rica. Geology 32, 957e960.
Lachniet, M.S., Asmerom, Y., Bernal, J.P., Polyak, V.J., Vazquez-Selem, L., 2013. Orbital pacing and ocean circulation-induced collapses of the Mesoamerican monsoon over the past 22,000 y. PNAS 110, 9255e9260.
Lane, C.S., Horn, S.P., Mora, C.I., Orvis, K.H., 2009. Late-Holocene paleoenvironmental change at mid-elevation on the Caribbean slope of the Cordillera Central, Dominican Republic: a multi-site, multi-proxy analysis. Quat. Sci. Rev. 28, 2239e2260.
Lasserre, G., 1961. La Guadeloupe: Etude Geographie. Union française d'impression.
Lea, D.W., Pak, D.K., Peterson, L.C., Hughen, K.A., 2003. Synchroneity of tropical and high-latitude Atlantic temperatures over the last glacial termination. Science 301, 1361e1364.
Lenoble, A., Angin, B., Huchet, J.-B., Royer, A., 2014. Seasonal insectivory of the Antillean fruit bat (Brachyphylla cavernarum). Carib. J. Sci. 48 (2e3), 127e131.
Lenoble, A., Queffelec, A., Bonnissent, D., Stouvenot, C., 2015. Rock art taphonomy in Lesser Antilles: study of wall weathering and engravings preservation in two precolumbian caves on Marie-Galante Island. In: Proceedings of the 26th IACA Congress, Puerto Rico.
Lenoble, A., Stouvenot, C., Courtaud, P., Grouard, S., Scalliet, M., Serrand, N., 2009. Formes et remplissages du karst littoral guadeloupeen. In: Vanara, N., Orthez, Douat M. (Eds.), Le karst, indicateur performant des environnements passes et actuels. ICN, pp. 226e233.
Leuenberger, M., Siegenthaler, U., Langway, C., 1992. Carbon isotope composition of atmospheric CO_2 during the last ice age from an Antarctic ice core. Nature 357, 488e490.
Leyden, B.W., 1995. Evidence of the younger dryas in Central America. Quat. Sci. Rev. 14, 833e839.
Makarov, M.I., 2009. The nitrogen isotopic composition in soils and plants: its use in environmental studies (a review). Eurasian Soil Sci. 42, 1335e1347.
Malaize, B., Bertran, P., Carbonel, P., Bonnissent, D., Charlier, K., Galop, D., Imbert, D., Serrand, N., Stouvenot, C., Pujol, C., 2011. Hurricanes and climate in the Caribbean during the past 3700 years BP. Holocene 21, 911e924.
Masson, D., Breuil, M., Breuil, A., 1990. Premier inventaire des chauves-souris de l'île de Marie-Galante (Antilles françaises). Mammalia 54, 656e658.
McCarthy, T.J., Henderson, R.W., 1992. Confirmation of Ardops nichollsi on MarieGalante, Lesser Antilles, and comments on other bats. Carib. J. Sci. 28 (1e2), 106e107.
McFarlane, D.A., Lundberg, J., Fincham, A.G., 2002. A late Quaternary paleoecological record from caves of southern Jamaica, West Indies. J. Cave Karst Stud. 64, 117e125.
Mizutani, H., Wada, E., 1988. Nitrogen and carbon isotope ratios in seabird rookeries and their ecological implications. Ecology 69, 340e349.
Mizutani, H., McFarlane, D.A., Kabaya, Y., 1992a. Carbon and nitrogen isotopic signatures of bat guanos as record of past environments. J. Mass. Spectrom. Soc. Jap 40, 67e82.
Mizutani, H., McFarlane, D.A., Kabaya, Y., 1992b. Nitrogen and carbon isotope study of bat guano core from Eagle Creek Cave, Arizona, USA. J. Mass. Spectrom. Soc. Jap. 40, 57e65.
Morrison, D.W., 1980. Efficiency of food utilization by fruit bats. Oecologia 45, 270e273.
Murphy, B.P., Bowman, D.M.J.S., 2006. Kangaroo metabolism does not cause the relationship between bone collagen $\delta^{15}N$ and water availability. Funct. Ecol. 20, 1062e1069.
Murphy, B.P., Bowman, D.M.J.S., 2009. The carbon and nitrogen isotope composition of Australian grasses in relation to climate. Funct. Ecol. 23, 1040e1049.
North Greenland Ice Core Project, 2004. High-resolution record of Northern Hemisphere climate extending into the last interglacial period. Nature 431, 147e151.

Onac, B.P., Forray, F.L., Wynn, J.G., Giurgiu, A.M., 2014. Guano-derived $d^{13}C$-based paleo-hydroclimate record from Gaura cu Musca Cave, SW Romania. Environ. Earth Sci. 71, 4061e4069.

Onac, B.P., Hutchison, S.M., Geanta, A., Forray, F.L., Wynn, J.G., Giurgiu, A.C., Coroiu, I., 2015. A 2500-year Late Holocene multi-proxy record of vegetation and hydrologic changes from a cave guano-clay sequence in SW Romania. Quat. Res. 83, 437e448. http://dx.doi.org/10.1016/j.ypres.2015.01.007.

Painter, M.L., Chambers, C.L., Siders, M., Doucett, R.R., Whitaker, J.J.O., Phillips, D.L., 2009. Diet of spotted bats (Euderma maculatum) in Arizona as indicated by fecal analysis and stable isotopes. Can. J. Zool. 87, 865e875.

Perez, L., Frenzel, P., Brenner, M., Escobar, J., Hoelzmann, P., Scharf, B., Schwalb, A., 2011. Late Quaternary (24e10 ka BP) environmental history of the Neotropical lowlands inferred from ostracodes in sediments of Lago Peten Itza, Guatemala.
J. Paleolimnol. 46, 59e74.

Peterson, L.C., Haug, G.H., 2006. Variability in the mean latitude of the Atlantic Intertropical Convergence Zone as recorded by riverine input of sediments to the Cariaco Basin (Venezuela). Palaeogeo. Paleoclim. Paleoecol. 234, 97e113.

Peterson, L.C., Haug, G.H., Hughen, K.A., Ro€hl, U., 2000. Rapid changes in the hydrologic cycle of the tropical Atlantic during the last glacial. Science 290, 1947e1951.

Portecop, J., 1982. Vegetation, Atals des Departements français d'Outre-Mer.III. La Guadeloupe. CNRS, Paris.

Pregill, G.K., Olson, S.L., 1981. Zoogeography of West Indian vertebrates in relation to Pleistocene climatic cycles. Annu. Rev. Ecol. Syst. 12, 75e98.

Pregill, G.K., Steadman, D.W., Watters, D.R., 1994. Late Quaternary Vertebrate Faunas of the Lesser Antilles: Historical Components of Carribbean Biogeography. Carnegie Museum of Natural History.

Prentice, I.C., Harrison, S.P., 2009. Ecosystem effects of CO_2 concentration: evidence from past climates. Clim. Past. 5, 297e307. http://dx.doi.org/10.5194/cp-5-2972009.

R Development Core Team, 2008. R: a Language and Environment for Statistical Computing. Vienna, Austria. http://www.R-project.org.

Rama-Corredor, O., Martrat, B., Grimalt, J.O., Lopez-Otalvaro, G.E., Flores, J.A., Sierro, F., 2015. Parallelisms between sea surface temperature changes in the western tropical Atlantic (Guiana Basin) and high latitude climate signals over the last 140 000 years. Clim. Past. 11, 1297e1311.

Reimer, P., Bard, E., Bayliss, A., Beck, J., Blackwell, P., Bronk Ramsey, C., Buck, C., Cheng, H., Edwards, R., Friedrich, M., Grootes, P., Guilderson, T., Haflidason, H., Hajdas, I., Hatte, C., Heaton, T., Hoffmann, D., Hogg, A., Hughen, K., Kaiser, K., Kromer, B., Manning, S., Niu, M., Reimer, R., Richards, D., Scott, E., Southon, J., Staff, R., Turney, C., Van der Plicht, J., 2013. IntCal13 and Marine13 radiocarbon age calibration curves 0e50,000 years cal BP. Radiocarbon 55, 1869e1887.

Rodet, J., 1987. La speleologie des îles calcaires de la Grande-Terre et de MarieGalante. In: Actes du 8e Congres national de la Societe Suisse de Spel eologie, Societe Suisse de Speleologie et Commission de Speleologie de la Societe Helvetique des Sciences Naturelles, Turgi. departement de la Guadeloupe, Petites Antilles, France, pp. 227e236.

Rodríguez-Duran, A., 2010. Bat assemblages in the West Indies: the role of caves. In: Fleming, T.H., Racey, P.A. (Eds.), Island Bats: Evolution, Ecology and Conservation. The University of Chicago Press, Chicago (IL), pp. 265e280.

Rousteau, A., Portecop, J., Rollet, B., 1996. Carte ecologique de la Guadeloupe. ONF, UAG, PNG, CGG, Jarry, Guadeloupe.

Royer, A., Queffelec, A., Charlier, K., Puech, E., Malaize, B., Lenoble, A., 2015. Seasonal changes in stable carbon and nitrogen isotope compositions of bat guano (Guadeloupe). Palaeogeo. Paleoclim. Paleoecol. 440, 524e532.

Salvarina, I., Yohannes, E., Siemers, B.M., Koselj, K., 2013. Advantages of using fecal samples for stable isotope analysis in bats: evidence from a triple isotopic experiment. Rapid Commun. Mass Spectrom. 27, 1945e1953.
Schmidt, M.W., Chang, P., Hertzberg, J.E., Them, T.R., Ji, L., Otto-Bliesner, B.L., 2012. Impact of abrupt deglacial climate change on tropical Atlantic subsurface temperatures. PNAS 109, 14348e14352.
Schmidt, M.W., Spero, H.J., Lea, D.W., 2004. Links between salinity variation in the Caribbean and North Atlantic thermohaline circulation. Nature 428, 160e163.
Schmitt, J., Schneider, R., Elsig, J., Leuenberger, D., Lourantou, A., Chappellaz, J., Ko€hler, P., Joos, F., Stocker, T.F., Leuenberger, M., 2012. Carbon isotope constraints on the deglacial CO_2 rise from ice cores. Science 336, 711e714.
Smith, B.N., Epstein, S., 1971. Two categories of $^{13}C/^{12}C$ ratios for higher plants. Plant Physiol. 47, 380e384.
Smith, B.N., Oliver, J., Mc Millan, C., 1976. Influence of carbon source, oxygen concentration, light intensity, and temperature on $^{13}C/^{12}C$ ratios in plant tissues. Bot. Gaz. 137, 99e104.
Soto-Centeno, J.A., Phillips, D.L., Kurta, A., Hobson, K.A., 2014. Food resource partitioning in syntopic nectarivorous bats on Puerto Rico. J. Trop. Ecol. 1e11.
Soto-Centeno, J.A., Rodriguez-Duran, A., Cortes, E., 2001. Erophylla sezekorni and Brachyphylla cavernarum diet of two Phyllostomid bats in Puerto Rico. Bat Res. News 42, 180e181.
Stevens, R.E., Hermoso-Buxan, X.L., Marín-Arroyo, A.B., Gonzalez-Morales, M.R., Straus, L.G., 2014. Investigation of Late Pleistocene and Early Holocene palaeoenvironmental change at El Miron cave (Cantabria, Spain): insights from carbon and nitrogen isotope analyses of red deer. Palaeogeo. Paleoclim. Paleoecol. 414, 46e60.
Stevens, R.E., Jacobi, R., Street, M., Germonpre, M., Conard, N.J., Münzel, S.C., Hedges, R.E.M., 2008. Nitrogen isotope analyses of reindeer (Rangifer tarandus), 45,000 BP to 9,000 BP: palaeoenvironmental reconstructions. Palaeogeo. Paleoclim. Paleoecol. 262, 32e45.
Stoetzel, E., Royer, A., Cochard, D., Lenoble, A., 2016. Late Quaternary changes in Bat palaeobiodiversity and palaeobiogeography under climatic and anthropogenic pressure: new insights from Marie-Galante, Lesser Antilles. Quat. Sci. Rev. 143, 150e174.
Stouffer, R.J., Yin, J., Gregory, J.M., Dixon, K.W., Spelman, M.J., Hurlin, W., Weaver, A.J., Eby, M., Flato, G.M., Hasumi, H., Hu, A., Jungclaus, J.H., Kamenkovich, I.V., Levermann, A., Montoya, M., Murakami, S., Nawrath, S., Oka, A., Peltier, W.R., Robitaille, D.Y., Sokolov, A., Vettoretti, G., Weber, S.L., 2006. Investigating the causes of the response of the thermohaline circulation to past and future climate changes. J. Clim. 19, 1365e1387.
Stouvenot, C., 2003. Cavites Naturelles Dans L'archipel Guadeloupeen. Prospection Thematique 2003. SRA DRAC Guadeloupe.
Stouvenot, C., 2005. Capesterre de Marie-Galante. Grotte Blanchard.
Notice scientifique page 28, Bilan scientifique 2005 SRA Guadeloupe. Direction Regionale des Affaires Culturelles de Guadeloupe, Basse-Terre Guadeloup e.
Street-Perrott, F.A., Hales, P.E., Perrott, R.A., Fontes, J.C., Switsur, V.R., Pearson, A., 1993. Late quaternary palaeolimnology of a tropical marl lake: Wallywash Great Pond, Jamaica. J. Paleolimnol. 9, 3e22.
Teeri, J.A., Stowe, L.G., 1976. Climatic patterns and the distribution of C4 grasses in North America. Oecologia 23, 1e12.
Tieszen, L.L., Reed, C.B., Bliss, N.B., Wylie, B.K., Delong, D.D., 1997. NDVI, C3 and C4 production, and distributions in Great Plains grassland land cover classes. Ecol. Appl. 7, 59e78.
Van de Water, P.K., Leavitt, S.W., Betancourt, J.L., 1994. Trends in stomatal density and $^{13}C/^{12}C$ ratios of Pinus flexilis needles during Last Glacial-Interglacial cycle. Science 264, 239e243.

Wang, Y.J., Cheng, H., Edwards, R.L., An, Z.S., Wu, J.Y., Shen, C.-C., Dorale, J.A., 2001. A high-resolution absolute-dated late Pleistocene monsoon record from Hulu Cave, China. Science 294, 2345e2348.

Wang, X., Auler, A.S., Edwards, R.L., Cheng, H., Ito, E., Wang, Y., Kong, X., Solheid, M., 2007. Millennial-scale precipitation changes in southern Brazil over the past 90,000 years. Geophys. Res. Lett. 34 http://dx.doi.org/10.1029/2007GL031149.

Widga, C., Colburn, M., 2015. Paleontology and paleoecology of guano deposits in Mammoth Cave, Kentucky, USA. Quat. Res. 83, 427e436.

Weldeab, S., 2012. Bipolar modulation of millennial-scale West African monsoon variability during the last glacial (75,000e25,000 years ago). Quat. Sci. Rev. 40, 21e29.

Wurster, C.M., McFarlane, D.A., Bird, M.I., 2007. Spatial and temporal expression of vegetation and atmospheric variability from stable carbon and nitrogen isotope analysis of bat guano in the southern United States. Geochim. Cosmochim. Acta 71, 3302e3310.

Wurster, C.M., Patterson, W.P., McFarlane, D.A., Wassenaar, L.I., Hobson, K.A., Athfield, N.B., Bird, M.I., 2008. Stable carbon and hydrogen isotopes from bat guano in the Grand Canyon, USA, reveal Younger Dryas and 8.2 ka events. Geology 36, 683e686.

Wurster, C.M., Bird, M.I., Bull, I.D., Creed, F., Bryant, C., Dungait, J.A., Paz, V., 2010a. Forest contraction in north equatorial Southeast Asia during the last Glacial Period. PNAS 107, 15508e15511.

Wurster, C.M., McFarlane, D.A., Bird, M.I., Ascough, P.I., Athfield, N.B., 2010b. Stable isotopes of subfossil bat guano as a long-term environmental archive: insights from a Grand Canyon cave deposit. J. Cave Karst Stud. 72, 111e121.

Yanes, Y., Romanek, C.S., 2013. Quaternary interglacial environmental stability in San Salvador Island (Bahamas): a land snail isotopic approach. Palaeogeo. Paleoclim. Paleoecol. 369, 28e40.

Ziegler, M., Jilbert, T., de Lange, G.J., Lourens, L.J., Reichart, G., 2008. Bromine counts from XRF scanning as an estimate of the marine organic carbon content of sediment cores. Geochem. Geophy. Geosy. 9, Q05009.

Appendix A. Supplementary data

Suppl. material S1: Materials and method for the mineralogical/pH supplementary information.

Mineralogical compositions from sediments were analyzed using X-ray diffraction on ground samples in a silicon calibrated PANalytical X'Pert diffractometer, using the K-Alpha 1 of a copper anticathode at 40 kV and 40 mA, from 8 to 80°. Minerals were identified using the JCPDS-ICDD database via the DIFFRACPLUS Eva software. TOPAS software allowed the quantification of mineralogical phases based on the Rietveld refinement method (1969). pH levels were measured from a suspension of 2 g of sediment in 10 g of water, using a pH meter calibrated with buffer solutions at pH 4 and 7 following the protocol described by Baize (2000). Energy Dispersive X-Ray Fluorescence (ED-XRF) analysis were conducted with an AMETEK Spectro X-Sort equipped with a tungsten X-ray tube (40 kV, 0,01 mA) for 60 seconds. Since there is no calibration for this kind of matrix, fundamental parameters algorithm has been used for concentration calculations of potassium, calcium, phosphorus and iron (e.g. Jenkins et al., 1995).

Results and discussion:

Eight authigenic minerals and five detrital minerals are found throughout the deposit (Table S1-1). This mineral composition is relatively typical of Caribbean caves (Onac et al., 2009).

Mineral	Formula	Origin
Hydroxylapatite	$Ca_5(PO_4)_3(OH)$	Authigenic phosphates
Whitlockite	$Ca_{18}Mg_2H_2(PO_4)_{14}$	
Tinsleyite	$KAl_2(PO_4)_2(OH),2H_2O$	
Leucophosphite	$KFe_2(PO_4)_2(OH),2H_2O$	
Taranakite	$(K_3Al_5(HPO_4)_6(PO_4)_2(H_2O)_{18}$	
Crandallite	$CaAl_3(PO_4)_2(OH)_5,H_2O$	
Gypse	$CaSO_4,2H_2O$	Authigenic sulfate

Calcite + Dolomite	$CaCO_3 + CaMg(CO_3)_2$	Detrital
Quartz	SiO_2	
Montmorillonite	$(Na,Ca)_{0.3}(Al,Mg)_2Si_4O_{10}(OH)_2,x(H_2O)$	
Labradorite	$(Ca,Na)(Al,Si)_4O_8$	
Halite	NaCl	Seaspray

Table S1.1 - List of minerals identified in the Blanchard cave infilling.

Sample	Sedimentary level	Square	Depth (mm)	K (% FP)	Ca (% FP)	P (% FP)	Fe (% FP)	pH	Mineralogical composition (%)											
									Hydroxylapatite	Whitlockite	Tinsleyite	Leucophosphite	Taranakite	Crandallite	Gypsum	Calcite + Dolomite	Quartz	Montmorillonite	Plagioclase	Biotite	Halite
GB 05.01	1	H33	-128	1.4	23	10.2	1.2	5.9	15	67	14				3						
GB 05.02	1	H33	-230	-	-	-	-	-	10	73	11									4	2
GB 07.07-08.29	2	H33	-333	1.3	17	8.3	1.2	5.2	17	59	16				4						4
GB 08.06	3	H33	-408	1.2	21	10.4	1.3	5.1	14	66	11		2								5
GB 08.05	3	H33	-483	0.8	21	9.4	0.9	5	15	82											3
GB 08.07	3	H33	-517	0.8	25	11.4	0.6	-	12	82			2								3
GB 05.03	4	H33	-666	0.5	24	2.4*	1.1	8.4	6	9						75		10			
GB 05.04	4	H33	-752	0.5	27	2.3*	0.9	8.5	2	6						87	1	4			
GB 07.09-08.34	5	H33	-909	0.5	22	8.9	0.8	8.2	17	75	4							1			
GB 07.08-08.35	5	H33	-975	0.6	20	7.8	1.2	8.3	12	80	3							1			3
GB 07.02	6	H33	-1051	0.6	26	10.6	0.6	6.2	17	64	5				7	1	5	1			
GB 08.08	6	H33	-1175	0.5	22	7.0	1.1	-	28	40					7	20	2	3			
GB 08.09	7	H33	-1275	0.5	23	7.4	1.4	8.2	32	46					2	14	1	3			
GB 08.11	8	H33	-1357	0.4	26	10.6	1.2	8	34	55					7	2	1	1			
GB 11.01	8	H33	-1414	0.4	24	9.7	1.3	7.8	28	66					4		1	1			
GB 11.02	8	H33	-1541	0.4	25	10.0	1.1	7.8	33	60					4			2			
GB 08.13	8	H33	-1609	0.4	27	10.8	0.7	7.7	29	65					5			1			
GB 08.14	8	H33	-1703	0.5	22	9.5	1.8	7.5	20	71					4		2	3			
GB 08.15	9	H33	-1797	0.6	22	9.2	2.3	8.1	26	68							1	4			
GB 08.16	10	H33	-1881	0.5	24	10.1	1.9	7.5	40	45					5		3	4			
GB 08.17	10	H33	-1959	0.4	25	9.9	1.7	7.8	59	25					10		3	2			
GB 14.05	11	H33	-2238	1.4	19	14.5	3.0	7.1	55	22	6	7			2	2	2	4			
GB 14.13	11	H31	-2254	1.3	28	13.4	2.5	6.8	57	23	10	6				2	1	2			
GB 14.07	12	H33	-2352	2.0	13	10.7	4.3	5.8	50	8	12	12				1	7	7			
GB 14.17	12	H31	-2399	2.2	15	11.2	3.6	6.8	56	7	16	10			1	2	4	4			
GB 14.08	Reaction layer	H33	-2410	0.5	27	12.5	2.2	6.6	78	10	5			3		2	2				
GB 14.09	Reaction layer	H33	-2422	-	-	-	-	7	51	49											
GB 14.20	Reaction layer	H31	-2710	0.3	37	16.3	0.4	-	65	13							3	14	5		

Table S1.2 – Major element proportion derived from XRF analysis, pH and mineralogical composition of samples from the Blanchard Cave deposit. Symbol (*) indicates overestimated phosphorus value as a consequence of calcium escape line artifact.

The proportion of gypsum is relatively low (Table S1-2) compared to other caves on the island (Lenoble et al., 2009). Detrital elements are mainly derived forms connected to the weathering of the surrounding rock. While these elements are more significant in the lower part of the cave fill, evaporite components, such as halite with a seaspray origin, are abundant in the upper part of the deposit (Table S1-2), in relation with the Holocene sea-level highstand.

The most abundant minerals are constituted by authigenic phosphates derived from biological inputs (Hill and Forti, 1997), apart from the level 4 where carbonates minerals dominated and phosphates are rare, due to this level's short period of formation as well as the origin of the material (limestone debris, *cf*. main text).

Phosphates were found as minerals formed by reactions with clays derived from the surrounding limestone. Potassium aluminium (tinsleyite) or iron-potassium forms (leucophosphite) are present but the majority of minerals are calcium and calcium-magnesium phosphates (hydroxylapatite and whitelockite, respectively). These latter minerals are produced by reactions with calcium or magnesium-rich sediment connected to the degradation of the host rock. Their occurrence indicates a low degree of sediment weathering (Karkanas and al., 1999), which is also evident in the high levels of pH measured through the deposit (Table S1-2). The low diagenetic transformation of the sediment indicated by phosphate minerals supports phosphate input by low trophic-level animals, such as frugivorous bats (Shahack-Gross et al., 2004). The low variations of both mineral assemblages and phosphate abundance measurements throughout the deposit suggest no significant change in biogenic

source related to a shift in trophic level, apart from the level 11. Indeed, this level presents a phosphorous content as high as those from the reaction layer, and also a high proportion of the insectivorous bat *Tadarida brasiliensis*, which is very different from other levels (Stoetzel *et al.*, 2016). It is noteworthy that the isotopic ratio of this bioturbated level obtained from one averaged sample does not depart from surrounding values. With the possible exception of this level, all these evidenced combined with the observation of fragmented vegetal tissues and the high level of organic matter in the sediment point to the deposit being primarily formed of fruit-bat guano.

References:

Baize, D., 2000. Guide des analyses en pédologie: 2e édition, revue et augmentée. Editions Quae.

Hill, C.A., Forti, P., 1997. Cave minerals of the world, second edition: Hunstville, Alabama, National Speleology Society, 463 p.

Jenkins, R., Gould, R.W., Gedcke, D., 1995. Quantitative X-ray spectrometry. CRC Press, New York, 491 p.

Karkanas, P., Kyparissi-Apostolika, N., Bar-Yosef, O., Weiner, S., 1999. Mineral assemblages in Theopetra, Greece: a framework for understanding diagenesis in a prehistoric cave. Journal of Archaeological Science 26, 1171-1180.

Lenoble, A., Stouvenot, C., Courtaud, P., Grouard, S., Scalliet, M., Serrand, N., 2009. Formes et remplissages du karst littoral guadeloupéen, in Vanara, N. and Douat, M., eds, Le karst, indicateur performant des environnements passés et actuels, Karstologia Mémoire, v. 17, p. 226-233.

Onac, B.P., Sumrali, J., Mylroie, J.E., Kearns, J., 2009. Cave Minerals of San Salvador Island, Bahamas: Tampa, University of South Florida Tampa library, Environmental Sustainability Publications, 70 p.

Rietveld, H., 1969. A profile refinement method for nuclear and magnetic structures. Journal of applied Crystallography 2, 65-71.

Shahack-Gross, R., Berna, F., Karkanas, P., Weiner, S., 2004. Bat guano and preservation of

archaeological remains in cave sites. Journal of Archaeological Science 31, 1259–1272.

Suppl. material S2: List of samples coming from the Blanchard Cave that have been analyzed for their carbon and nitrogen isotope compositions and reported along their sampling depth (mm), their nomenclature of sedimentary levels, and their mean, minimum and maximum geological ages calculated from the age-depth model explained in the text (see paragraph 3.2) with IntCal13. Isotopic ratios are also accompanied by the assumed CO_2 content (ppm) and carbon isotope ratios of the contemporaneous atmosphere, extracted from Ahn and Brook (2008) and Schmitt et al. (2012), respectively.

References:

Ahn, J., Brook, E.J., 2008. Atmospheric CO_2 and climate on millennial time scales during the last glacial period. Science 322, 83-85.

Schmitt, J., Schneider, R., Elsig, J., Leuenberger, D., Lourantou, A., Chappellaz, J., Köhler, P., Joos, F., Stocker, T.F., Leuenberger, M., 2012. Carbon isotope constraints on the deglacial CO_2 rise from ice cores. Science 336, 711-714.

Sample names	Depth (mm)	Sedimentary levels	Age from linear model (BP)	Max 99% - age from linear model (BP)	Min 99% - age from linear model (BP)	$\delta^{13}C$ (V-PDB)	S.D. $\delta^{13}C$	$\delta^{15}N$ (AIR)	S. D. $\delta^{15}N$	$\delta^{13}C$ atmosphere	$[CO_2]$ (ppm)	$\delta^{13}C$ corrected
Modern	-	Modern	-	-	-	-27	0.2	11.1	0.1	-8	380	-27.3
P13	573	3	10622	9810	10914	-25.6	-	18	-	-6.6	265.4	-25.6
P15	578	3	10699	9890	10989	-25.4	-	18.1	-	-6.6	266.4	-25.4
P17	583	3	10775	9970	11064	-25.5	-	18.8	-	-6.6	267.4	-25.6
P19	588	3	10852	10051	11140	-25.4	-	19	-	-6.6	268.3	-25.5
P21	594	3	10944	10147	11230	-25.6	-	18.3	-	-6.6	269.5	-25.8
P23	598	3	11006	10211	11290	-25.3	-	18.6	-	-6.6	270.3	-25.4
P25	603	3	11082	10292	11366	-25.3	-	18.5	-	-6.6	269.9	-25.2
P27	608	3	11159	10372	11441	-25.2	-	18	-	-6.6	269.1	-25.2
P31	615	3	11267	10485	11546	-24.8	-	18.1	-	-6.6	268.0	-24.8
P33	618	3	11313	10533	11591	-24.9	0.1	16.2	0.2	-6.6	267.6	-24.8
P35	622	3	11374	10597	11652	-24.8	0	17.5	0.1	-6.6	266.9	-24.7
P37	625	3	11420	10645	11697	-24.9	-	17.6	-	-6.6	266.5	-24.8

P39	629	3	11481	10708	11758	-24.7	-	18.4	-	-6.6	265.8	-24.5
P41	632	3	11527	10755	11804	-24.8	-	18.4	-	-6.7	265.4	-24.6
P43	636	3	11589	10818	11866	-24.6	-	18.1	-	-6.7	264.7	-24.4
P45	641	3	11666	10897	11942	-24.8	-	17.4	-	-6.7	263.9	-24.6
P47	646	3	11742	10977	12018	-24.8	-	17.5	-	-6.7	264.3	-24.6
P49	651	3	11819	11057	12094	-25.1	-	17.1	-	-6.7	262.6	-24.8
P51	656	3	11896	11137	12168	-25	-	16.1	-	-6.7	261.0	-24.9
P53	661	3	11973	11217	12245	-25.2	0	15.3	0.1	-6.7	259.3	-25.0
P55	666	3	12049	11297	12323	-25.1	0.1	14.9	0.1	-6.7	258.4	-24.9
P57	671	3	12126	11377	12398	-25.2	0	15.1	0.1	-6.7	256.0	-24.9
P59	676	3	12203	11457	12473	-24.9	0.1	15.1	-	-6.7	253.6	-24.6
P61	682	3/4	12295	11553	12564	-24.7	-	15.1	-	-6.7	250.8	-24.3
P63	984	5	12341	11601	12609	-25.1	0.1	16.4	0	-6.7	241.5	-24.5
P65	990	5	12433	11696	12699	-25.5	0.1	18	0.1	-6.7	240.2	-24.9
P67	995	5	12510	11776	12775	-25	-	20.3	-	-6.7	239.2	-24.4
P69	1000	5	12587	11856	12850	-24.7	-	20.7	-	-6.7	238.1	-24.1
P71	1005	5	12663	11936	12925	-24.1	-	20.9	-	-6.7	237.1	-23.5
P73	1009	5	12725	12000	12986	-23.6	-	21.6	-	-6.7	235.0	-22.9
P75	1014	5	12802	12080	13062	-23.2	-	21.8	-	-6.7	236.7	-22.5
P77	1018	5	12863	12144	13122	-22.9	-	22	-	-6.7	238.1	-22.3
P79	1023	5	12940	12224	13197	-22.4	0	22.2	0.2	-6.6	238.0	-21.8
P81	1028	5	13016	12304	13273	-22.2	-	21.8	-	-6.6	238.0	-21.6
P83	1033	5	13093	12384	13348	-21.8	-	21.8	-	-6.6	238.2	-21.2
P85	1037	5	13155	12448	13409	-21.5	-	21.3	-	-6.6	238.9	-20.9
P87	1042	5	13231	12528	13484	-21.1	-	21	-	-6.6	239.7	-20.6
P89	1047	5	13308	12608	13560	-21.1	-	21.4	-	-6.6	240.6	-20.5
P91	1052	5	13385	12688	13636	-20.9	-	21.3	-	-6.6	241.4	-20.4
P93	1057	5	13462	12768	13712	-21	-	21.5	-	-6.6	240.8	-20.5
P95	1063	5	13554	12864	13803	-20.8	0.1	21	0.2	-6.6	240.4	-20.3
P97	1067	5	13615	12928	13864	-20.8	0.1	21.6	0.1	-6.6	240.1	-20.2
P99	1071	5	13677	12992	13925	-20.7	-	21.7	-	-6.6	239.8	-20.1
P101	1077	5	13769	13088	14016	-20.5	-	21.8	-	-6.6	239.4	-19.9
P103	1082	5	13845	13168	14092	-20.4	-	21.6	-	-6.6	239.0	-19.8
P105	1087	5	13922	13247	14169	-20.5	-	21.4	-	-6.7	238.6	-19.9
P107	1092	5	13999	13327	14245	-20.4	-	21.2	-	-6.7	238.3	-19.8
P109	1097	5	14076	13407	14321	-20.5	-	21.5	-	-6.7	237.9	-19.9
P111	1102	5	14152	13487	14397	-20.5	-	21.5	-	-6.7	237.6	-19.9
P113	1107	5	14229	13567	14474	-20.5	0.1	21.8	0.2	-6.7	237.2	-19.8
P388	1164	6	15104	14481	15351	-20.2	-	22.7	-	-6.3	224.5	-19.7
P389	1214	6	15872	15281	16121	-20.4	0	22	0.1	-6.4	210.0	-19.6
P390	1264	7	16639	16077	16894	-21.9	-	17.4	-	-6.4	192.0	-20.7
P391	1314	7	17407	16869	17675	-23.3	0.3	13.2	0.3	-6.4	188.0	-22.0
P393	1414	7	18942	18445	19228	-23.2	0.1	12.1	0	-6.4	188.0	-21.8
P115	1452	8	19525	19050	19819	-22.2	0	15.1	0.2	-6.5	191.2	-20.8
P117	1457	8	19602	19130	19896	-22.6	0	13	0.3	-6.5	191.0	-21.3
P119	1460	8	19648	19177	19942	-23.4	0	11.3	0.3	-6.5	190.8	-22.0

P121	1465	8	19724	19257	20019	-23.9	0	9.3	-	-6.5	190.6	-22.5
P123	1470	8	19801	19337	20096	-23.3	0	12	0.2	-6.5	190.6	-22.0
P125	1475	8	19878	19417	20175	-23.1	-	12	-	-6.5	191.1	-21.8
P127	1480	8	19955	19496	20254	-23.1	0	12	0.2	-6.5	192.0	-21.7
P129	1485	8	20031	19576	20332	-23.8	0	9.6	0.1	-6.5	194.2	-22.5
P131	1490	8	20108	19656	20411	-24.1	0.1	8.4	-	-6.4	197.6	-22.9
P133	1495	8	20185	19735	20490	-24.3	0.1	8.8	0.1	-6.4	201.1	-23.1
P135	1500	8	20262	19816	20568	-24.2	0	9.7	0	-6.4	203.9	-23.1
P137	1505	8	20338	19896	20647	-24.1	0	10.3	0.1	-6.4	205.2	-23.0
P139	1510	8	20415	19975	20726	-24.2	0	10.9	-	-6.4	203.9	-23.1
P141	1515	8	20492	20054	20804	-24.2	-	11	-	-6.4	200.1	-23.1
P143	1520	8	20569	20134	20883	-24.4	-	11.1	-	-6.4	196.0	-23.1
P145	1525	8	20645	20213	20962	-24.4	0.1	10.8	-	-6.4	193.9	-23.1
P147	1530	8	20722	20292	21040	-24.4	-	10.7	-	-6.4	194.0	-23.1
P149	1535	8	20799	20371	21119	-24.4	-	11.1	-	-6.4	195.2	-23.2
P151	1540	8	20876	20452	21198	-24.5	0	12.3	0.1	-6.4	196.8	-23.3
P153	1545	8	20952	20533	21277	-24.6	0	14.3	0.1	-6.4	198.0	-23.4
P155	1550	8	21029	20612	21355	-24.7	-	15.1	-	-6.4	198.5	-23.5
P157	1555	8	21106	20692	21434	-24.6	-	15.5	-	-6.4	198.5	-23.4
P159	1560	8	21183	20772	21513	-24.5	0	15.7	-	-6.4	198.2	-23.3
P161	1565	8	21259	20851	21591	-24.5	-	14.9	-	-6.4	197.6	-23.3
P163	1570	8	21336	20931	21669	-24.5	0	14.2	-	-6.4	196.9	-23.3
P165	1575	8	21413	21011	21747	-24.6	-	14.1	-	-6.4	196.3	-23.4
P167	1580	8	21490	21089	21825	-24.7	0	14.2	-	-6.4	195.9	-23.4
P169	1585	8	21567	21166	21903	-24.8	-	14.6	-	-6.4	195.8	-23.5
P171	1590	8	21643	21244	21981	-24.6	0	14.8	-	-6.4	196.1	-23.4
P173	1595	8	21720	21325	22059	-24.6	-	14.9	-	-6.4	196.7	-23.4
P175	1600	8	21797	21404	22137	-24.6	-	14.6	-	-6.4	197.5	-23.4
P177	1605	8	21874	21482	22216	-24.6	0	13.6	0.3	-6.4	198.3	-23.5
P179	1610	8	21950	21561	22294	-24.7	0	12.5	0.2	-6.4	199.1	-23.6
P181	1615	8	22027	21640	22372	-24.6	0	10.7	-	-6.4	199.7	-23.4
P183	1620	8	22104	21719	22450	-24.4	0	9.2	-	-6.4	200.1	-23.2
P185	1625	8	22181	21797	22529	-24.3	0	8.6	-	-6.4	200.0	-23.1
P187	1628	8	22227	21844	22577	-24.4	0	10.8	0.4	-6.4	199.7	-23.3
P191	1640	8	22411	22032	22767	-24.1	-	8.4	-	-6.4	197.0	-22.9
P193	1645	8	22488	22110	22846	-24.2	-	8	-	-6.4	195.7	-22.9
P195	1650	8	22564	22189	22924	-24.1	-	7.7	-	-6.4	194.5	-22.8
P197	1655	8	22641	22267	23002	-24.1	-	7.8	-	-6.4	193.7	-22.8
P199	1660	8	22718	22346	23080	-24.1	-	7.7	-	-6.4	193.2	-22.8
P201	1665	8	22795	22424	23158	-24.1	-	8	-	-6.4	192.9	-22.8
P203	1670	8	22871	22501	23236	-24.1	-	8	-	-6.4	193.0	-22.8
P205	1675	8	22948	22580	23314	-24.1	-	8.1	-	-6.4	193.2	-22.8
P207	1680	8	23025	22657	23392	-24.2	-	8.2	-	-6.4	193.6	-23.0
P209	1685	8	23102	22733	23470	-24.2	0.1	8.2	0.2	-6.4	194.1	-22.9
P211	1690	8	23178	22810	23548	-24.2	0	9.4	0.1	-6.4	194.7	-22.9
P213	1695	8	23255	22885	23626	-24.1	0.1	10.1	0	-6.4	195.2	-22.9

P215	1700	8	23332	22961	23705	-24.2	-	13.1	-	-6.4	195.8	-23.0
P217	1705	8	23409	23039	23783	-24.3	-	15.1	-	-6.4	196.3	-23.1
P219	1710	8	23485	23116	23861	-24.2	-	15.6	-	-6.4	196.7	-23.0
P221	1715	8	23562	23192	23939	-24.3	-	16.4	-	-6.4	197.1	-23.2
P223	1720	8	23639	23269	24017	-24.4	-	17.5	-	-6.4	197.3	-23.2
P225	1725	8	23716	23345	24095	-24.4	-	17.8	-	-6.4	197.5	-23.2
P227	1730	8	23792	23423	24173	-24.3	-	18	-	-6.4	197.6	-23.2
P229	1735	8	23869	23501	24251	-24.4	-	18.2	-	-6.4	197.7	-23.2
P231	1740	8	23946	23577	24329	-24.4	-	18.4	-	-6.4	197.6	-23.2
P233	1745	8	24023	23652	24407	-24.5	0	17.9	-	-6.4	197.6	-23.3
P235	1750	8	24099	23728	24484	-24.4	-	18.4	-	-6.4	197.4	-23.2
P237	1754	8	24161	23789	24546	-24.4	-	17.7	-	-6.4	197.2	-23.2
P239	1759	8	24237	23865	24625	-24.5	-	17.8	-	-6.4	197.0	-23.3
P241	1765	8	24330	23957	24719	-24.5	-	17.4	-	-6.4	196.6	-23.3
P243	1770	8	24406	24033	24797	-24.3	-	17.9	-	-6.4	196.2	-23.1
P245	1775	8	24483	24110	24876	-24.4	-	17.7	-	-6.4	195.8	-23.2
P247	1780	8	24560	24186	24955	-24.5	-	17.8	-	-6.4	195.4	-23.2
P249	1785	8	24637	24263	25034	-24.6	0.1	17.1	0.1	-6.4	194.8	-23.4
P251	1790	8	24713	24339	25112	-24.9	0.1	16.9	0.6	-6.4	194.3	-23.6
P253	1795	8	24790	24416	25190	-24.4	0	17	-	-6.4	193.7	-23.2
P255	1800	8	24867	24492	25268	-24.4	0	16.9	-	-6.4	193.1	-23.1
P257	1806	8	24959	24584	25362	-24.2	0	16.3	-	-6.4	192.3	-22.9
P259	1812	8	25051	24676	25456	-24.2	-	16.1	-	-6.4	191.6	-22.9
P261	1815	8	25097	24721	25503	-24.3	-	16.2	-	-6.4	191.3	-23.0
P263	1820	8	25174	24797	25581	-24.2	-	15.6	-	-6.4	190.8	-22.9
P265	1826	8	25266	24887	25674	-24.1	-	16.2	-	-6.4	190.2	-22.8
P267	1832	8	25358	24976	25768	-24.2	-	16	-	-6.4	189.7	-22.8
P269	1840	8	25481	25096	25893	-24.1	-	15.4	-	-6.4	189.3	-22.7
P271	1844	8	25542	25156	25955	-23.9	-	16.1	-	-6.4	189.2	-22.5
P273	1848	8	25604	25216	26018	-23.7	0.1	15.5	0.3	-6.4	189.1	-22.3
P275	1850	8	25634	25246	26049	-23.3	-	16.1	-	-6.4	189.1	-21.9
P277	1855	8	25711	25321	26127	-23.1	0	17.2	0.1	-6.4	189.3	-21.7
P279	1860	8	25788	25400	26205	-22.8	0.1	17.7	0.1	-6.4	189.5	-21.5
P281	1865	8	25865	25475	26283	-22.8	-	18.5	-	-6.4	190.0	-21.4
P283	1870	8	25941	25550	26362	-22.6	-	18.7	-	-6.4	190.6	-21.3
P285	1875	8	26018	25624	26443	-22.8	0	18.4	0.2	-6.4	191.2	-21.5
P287	1880	8	26095	25698	26523	-22.7	0.1	18.5	0.2	-6.4	191.9	-21.4
P289	1885	8	26172	25773	26604	-22.8	0.1	18.5	0.1	-6.4	192.5	-21.5
P291	1890	8	26248	25849	26682	-22.9	0	18.4	0	-6.4	192.9	-21.6
P293	1895	8	26325	25924	26760	-22.8	-	17.8	-	-6.4	193.2	-21.6
P295	1900	8	26402	25999	26838	-22.8	-	17.6	-	-6.4	193.1	-21.5
P297	1905	8	26479	26074	26917	-22.6	-	16.6	-	-6.4	192.8	-21.3
P299	1910	8	26555	26150	26996	-22.5	0	17.4	0	-6.4	192.0	-21.2
P301	1915	8	26632	26224	27075	-22.2	0.1	16.5	-	-6.4	190.8	-20.8
P395	1991	9	27799	27365	28265	-22.5	0.1	11.7	0.1	-6.4	201.5	-21.4
P303	1996	10	27875	27440	28343	-24.3	-	10.1	-	-6.4	203.5	-23.3

P305	2002	10	27968	27529	28437	-24.5	-	9.6	-	-6.4	205.1	-23.4
P307	2007	10	28044	27604	28516	-24.8	-	9.5	-	-6.4	205.6	-23.8
P309	2012	10	28121	27679	28594	-24.8	-	9.3	-	-6.4	205.8	-23.8
P311	2017	10	28198	27754	28672	-24.7	-	9.3	-	-6.4	205.9	-23.7
P313	2023	10	28290	27844	28766	-24.4	-	10.2	-	-6.4	206.2	-23.4
P315	2027	10	28351	27904	28829	-24.9	-	9.5	-	-6.4	206.6	-23.9
P317	2032	10	28428	27979	28907	-24.3	-	9.3	-	-6.4	207.2	-23.3
P319	2037	10	28505	28054	28985	-24.1	-	9.5	-	-6.4	207.6	-23.1
P321	2042	10	28582	28128	29064	-23.9	-	10	-	-6.4	207.7	-22.9
P323	2047	10	28658	28203	29142	-23.9	-	10.3	-	-6.4	207.6	-22.9
P325	2052	10	28735	28277	29220	-24.3	0.2	10.4	0.3	-6.4	207.3	-23.3
P327	2057	10	28812	28351	29298	-23.9	-	10.8	-	-6.4	206.8	-22.9
P329	2062	10	28889	28425	29377	-23.7	-	11.1	-	-6.4	206.2	-22.7
P331	2067	10	28965	28500	29456	-23.7	-	10.4	-	-6.4	205.6	-22.7
P333	2072	10	29042	28574	29535	-23.8	-	11.1	-	-6.4	204.9	-22.8
P335	2077	10	29119	28649	29615	-23.8	-	10.4	-	-6.4	204.2	-22.7
P337	2082	10	29196	28723	29694	-24	-	10.1	-	-6.4	203.5	-22.9
P339	2087	10	29272	28797	29773	-24.2	-	9.5	-	-6.4	202.7	-23.1
P341	2092	10	29349	28871	29853	-24.3	-	9.1	-	-6.4	202.0	-23.3
P343	2097	10	29426	28945	29932	-24.3	-	8.8	-	-6.4	201.2	-23.2
P345	2102	10	29503	29019	30011	-24.4	-	8.8	-	-6.4	200.4	-23.3
P347	2107	10	29579	29093	30090	-24.7	-	8.7	-	-6.4	199.7	-23.5
P349	2112	10	29656	29168	30170	-24.6	-	8.1	-	-6.4	199.0	-23.5
P351	2117	10	29733	29243	30249	-24.8	-	8.5	-	-6.4	198.3	-23.7
P353	2122	10	29810	29318	30329	-24.8	-	8.1	-	-6.4	197.7	-23.6
P355	2127	10	29886	29393	30408	-25	-	8.4	-	-6.4	197.2	-23.8
P357	2132	10	29963	29468	30488	-25.1	-	8.3	-	-6.4	196.8	-23.9
P359	2137	10	30040	29542	30567	-25.1	-	7.6	-	-6.4	196.4	-23.9
P361	2142	10	30117	29617	30646	-24.8	-	8.1	-	-6.4	196.0	-23.6
P363	2147	10	30193	29692	30726	-25	-	8	-	-6.4	195.6	-23.8
P365	2152	10	30270	29767	30805	-24.9	-	8	-	-6.4	195.2	-23.7
P367	2157	10	30347	29842	30884	-25.1	-	7.7	-	-6.4	194.8	-23.8
P369	2162	10	30424	29917	30964	-25.1	-	7.9	-	-6.4	194.5	-23.8
P371	2167	10	30500	29991	31043	-25.1	-	7.5	-	-6.4	194.1	-23.8
P373	2172	10	30577	30066	31122	-25	-	8.5	-	-6.4	193.8	-23.8
P375	2182	10	30731	30215	31282	-24.8	-	7.5	-	-6.4	193.6	-23.6
P377	2188	10	30823	30305	31378	-24.9	-	8.7	-	-6.4	193.7	-23.7
P379	2193	10	30899	30380	31457	-25.1	-	8.3	-	-6.4	193.9	-23.9
P381	2199	10	30992	30470	31553	-25.1	-	8.4	-	-6.4	194.5	-23.9
P383	2208	10	31130	30605	31696	-25.1	-	8.2	-	-6.4	196.0	-23.9
P385	2214	10	31222	30695	31791	-25.2	-	8	-	-6.4	197.3	-24.1
P387	2220	10	31314	30783	31886	-25.3	-	7.7	0.2	-6.4	198.8	-24.2
P397	2229	10	31452	30917	32030	-25.2	-	7.7	-	-6.4	200.8	-24.1
P399	2237	10	31575	31036	32157	-25.4	-	7.5	-	-6.4	202.3	-24.3
P401	2243	10	31667	31125	32252	-25	-	7.5	-	-6.4	202.9	-24.0
P403	2250	10	31774	31230	32363	-24.9	-	7.5	-	-6.4	203.3	-23.9

P405	2261	10	31943	31394	32538	-24.8	-	6.8	-	-6.4	203.5	-23.7
P407	2272	10	32112	31558	32713	-24.7	-	7.8	-	-6.4	204.1	-23.6
P409	2279	10	32220	31663	32825	-24.4	-	7.2	-	-6.4	203.8	-23.3
P411	2287	10	32342	31782	32953	-24.1	-	-	-	-6.4	205.5	-23.1
P413	2350	11	33309	32714	33955	-24.7	-	-	-	-6.4	208.0	-23.7
P443	2421	12	34399	33764	35093	-23.7	-	16	-	-6.4	211.9	-22.8
P445	2426	12	34476	33838	35174	-23.4	0	17	0.3	-6.4	213.0	-22.6
P447	2435	12	34614	33971	35318	-22.2	0.1	16.9	0.2	-6.4	212.4	-21.3
P449	2440	12	34691	34045	35398	-20.2	0.1	18.5	-	-6.4	211.0	-19.3
P451	2446	12	34783	34133	35494	-19.8	-	-	-	-6.4	209.1	-18.8
P453	2453	12	34890	34238	35606	-22.2	0.1	-	-	-6.4	207.2	-21.2
P455	2460	12	34998	34343	35717	-23.1	-	-	-	-6.4	206.6	-22.1
P457	2466	12	35090	34432	35813	-23.4	-	10.8	-	-6.4	207.3	-22.4
P459	2471	12	35167	34507	35893	-23.8	-	10	-	-6.4	208.3	-22.9
P461	2476	12	35244	34582	35972	-24.3	-	9.2	-	-6.4	209.4	-23.4
P463	2480	12	35305	34642	36034	-24.2	-	8.8	-	-6.4	210.1	-23.3
P465	2487	12	35412	34746	36144	-24.3	-	8.6	-	-6.4	210.7	-23.4
P467	2494	12	35520	34851	36254	-24.3	-	8.7	-	-6.4	210.7	-23.4
P469	2499	12	35597	34926	36333	-24.7	-	-	-	-6.4	210.4	-23.8
P471	2504	12	35673	35001	36411	-24.8	-	-	-	-6.4	210.0	-23.9
P473	2509	12	35750	35075	36491	-24.9	-	-	-	-6.4	209.4	-24.0
P475	2514	12	35827	35150	36570	-25	-	-	-	-6.4	208.9	-24.0
P477	2520	12	35919	35240	36666	-24.9	-	7.7	-	-6.4	208.3	-24.0
P479	2528	12	36042	35360	36794	-25	-	7.4	-	-6.4	207.8	-24.0
P481	2534	12	36134	35449	36889	-25.1	-	6.4	-	-6.4	207.8	-24.1
P483	2539	12	36211	35524	36969	-25.3	-	6	-	-6.4	208.1	-24.4
P485	2544	12	36287	35599	37049	-25.1	-	-	-	-6.4	208.7	-24.2
P487	2550	12	36379	35689	37145	-25.2	-	6.3	-	-6.4	209.6	-24.3
P489	2555	12	36456	35763	37226	-25	0.1	6.9	0	-6.4	210.4	-24.1
P491	2563	12	36579	35883	37355	-25.6	-	-	-	-6.4	211.6	-24.7
P493	2572	12	36717	36016	37499	-25.7	-	6.4	-	-6.4	212.7	-24.8
P495	2582	12	36871	36165	37658	-25.3	-	7	-	-6.4	213.3	-24.4
P497	2590	12	36993	36284	37786	-25.2	-	7.6	-	-6.4	213.7	-24.4
P499	2597	12	37101	36387	37899	-25.2	-	7.7	-	-6.4	214.5	-24.3
P501	2607	12	37254	36536	38059	-25.1	-	-	-	-6.4	216.0	-24.3
P503	2614	12	37362	36640	38171	-24.9	-	8.1	-	-6.4	216.9	-24.1
P505	2621	12	37469	36744	38283	-24.6	-	-	-	-6.4	217.5	-23.8
P507	2629	12	37592	36863	38411	-24.6	-	-	-	-6.4	217.3	-23.8
P509	2639	12	37746	37011	38572	-24.3	-	-	-	-6.4	216.4	-23.5
P511	2648	12	37884	37145	38716	-24.5	-	-	-	-6.4	215.9	-23.6
P513	2657	12	38022	37278	38860	-24.3	-	-	-	-6.4	216.5	-23.5
P515	2664	12	38129	37382	38972	-24.5	0.1	-	-	-6.4	217.6	-23.7
P517	2671	12	38237	37486	39085	-24.4	-	-	-	-6.4	217.6	-23.6
P519	2677	12	38329	37575	39181	-24.8	-	-	-	-6.4	215.6	-23.9
P521	2684	12	38436	37679	39293	-24.5	-	-	-	-6.4	211.9	-23.6
P523	2689	12	38513	37753	39373	-24.9	-	10.1	-	-6.4	211.1	-24.0

P525	2695	12	38605	37842	39469	-24.8	-	-	-	-6.4	212.7	-24.0
P527	2702	12	38713	37946	39581	-25	-	-	-	-6.4	214.8	-24.2
P529	2709	12	38820	38050	39693	-24.9	-	-	-	-6.4	213.1	-24.0
P531	2713	12	38881	38110	39757	-24.7	-	-	-	-6.4	211.1	-23.8
P533	2718	12	38958	38184	39836	-25.2	-	9.2	-	-6.4	208.6	-24.3
P535	2724	12	39050	38273	39931	-25.2	-	9.5	-	-6.4	207.3	-24.2
P537	2731	12	39158	38377	40042	-25.5	-	9.9	-	-6.4	208.7	-24.5
P539	2738	12	39265	38481	40153	-25.5	-	10	-	-6.4	211.5	-24.6
P541	2746	12	39388	38600	40280	-25.2	-	10.2	-	-6.4	214.5	-24.4
P543	2753	12	39495	38703	40391	-25.3	-	10.2	-	-6.4	212.5	-24.4
P545	2760	12	39603	38807	40502	-25.4	-	10.7	-	-6.4	204.2	-24.4
P547	2769	12	39741	38941	40645	-25.2	-	10.6	-	-6.4	200.6	-24.1
P549	2778	12	39879	39075	40788	-24.9	-	-	-	-6.4	202.9	-23.9